# CHAPTER 1

# AUTOMATED IMAGE SEGMENTATION: ISSUES AND APPLICATIONS

Alain Pitiot[1], Hervé Delingette[2], Paul M. Thompson[3]

[1] *Mirada Solutions, Ltd., Oxford, UK*
[2] *EPIDAURE Laboratory, INRIA, Sophia Antipolis, France*
[3] *Laboratory of Neuro Imaging, UCLA School of Medicine, Los Angeles, USA*
*E-mail: apitiot@loni.ucla.edu*

The explosive growth in medical imaging technologies has been matched by a tremendous increase in the number of investigations centered on the structural and functional organization of the human body. A pivotal first step towards elucidating the correlation between structure and function, accurate and robust segmentation is a major objective of computerized medicine. It is also a substantial challenge in view of the wide variety of shapes and appearances that organs, anatomical structures and tissues can exhibit in medical images.

This chapter surveys the actively expanding field of medical image segmentation. We discuss the main issues that pertain to the remarkably diverse range of proposed techniques. Among others, the characteristics of a suitable segmentation paradigm, the introduction of *a priori* knowledge, robustness and validation are detailed and illustrated with relevant techniques and applications.

## 1. Introduction

Imaging technologies have undergone fast paced developments since the early days of anatomy. Magnetic resonance imaging (MRI), computer-assisted tomography (CT), positron emission tomography (PET) and an increasing number of other techniques (see Figure 1) now permit precise analysis of *post-mortem* tissue and non-invasive exploration of living organisms. They can elucidate the structures of organs and cells, observe and help understand their function, and give clinicians the means to monitor their dysfunctions, or assist in the removal of pathologies.

A deeper understanding of both the anatomical characteristics of the tissues and organs of the human body (or, more precisely, of the sub-structures we distinguish within them) and of their inter-relationships is crucial in diagnostic and interventional medicine. The need, shared across many levels of description, for such correlation between structure and function is exemplified by the vast number of studies analysing cortical structures (in populations with a particular disease [127], through the developmental cycle [16] or comparing normal and diseased subjects [189]), quantifying tissue loss, gain or structure volumes [94,55], or aiming for automated

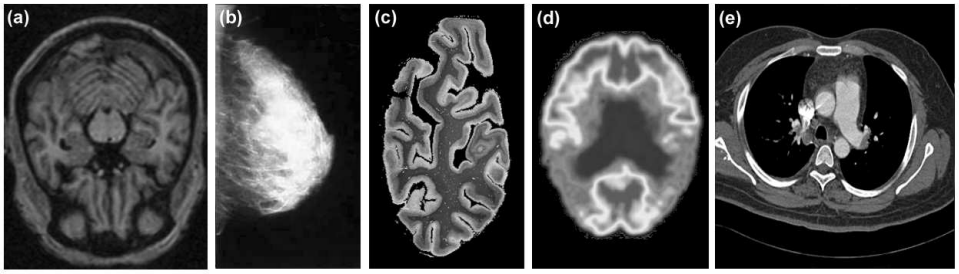


Fig. 1. A collection of imaging modalities: (a) MR image of the human brain, (b) digital mammogram, (c) myelin-stained histological section of the human visual cortex, (d) PET image of the human brain, (e) CT scan of the chest.

diagnosis of disease [185,176], among others.

While qualitative analysis may sometimes be sufficient for diagnosis, quantitative analysis, for which segmentation and labeling are absolute prerequisites, is necessary for a variety of applications: longitudinal monitoring of disease progression or remission [72,157], pre-operative evaluation and surgical planning [78,90,6], radiotherapy treatment planning [131] or statistical analysis of anatomic variability [38,193].

Even so, accurate segmentation of anatomical structures and tissues in medical images is especially challenging, given the wide variety of shapes, sizes and appearances they can present. Still the delineation process calls for high precision as the quality of the analysis generally depends on how accurately the various structures are identified. For instance, given the corpus callosum's key role as the primary cortical projection system, regional analysis of its structure is important in assessing several neurological disorders (Alzheimer's disease, vascular dementia, dysplasias). Nonetheless, subtle variations in shape, relative to a mean callosal delineation, are observed between and within patient and control groups, and this makes it difficult to detect and classify abnormal structural patterns. As a result, intense debate still rages on whether different callosal regions undergo selective changes in each of these disease processes and whether these are systematic differences in neuropsychiatric disorders such as autism or schizophrenia. These controversies may be alleviated by precise and reliable segmentations, applied to large image databases.

Segmentation has traditionally been tackled by human operators. However the many drawbacks of manual delineation (lack of reproducibility, *a priori* biases, lack of sufficient resources to handle ever-growing databases) favor the use of automated methods. Nonetheless, to reach the desired accuracy, many difficulties must be overcome: input images may be noisy, poorly contrasted and full of "decoys" (many structures are similar in shape or intensity), the target structures may be highly variable in geometry, etc.

We propose in this chapter an overview of the ever-expanding palette of automated segmentation techniques applied to biomedical images. Remarkably, the

diversity of the developed techniques is more than matched by the variety of the objectives (disease diagnosis, surgical planning, atlas building, etc.), of the segmentation targets and of the input imaging modalities, with substantially different hypotheses and requirements for each of them. Rather than arbitrarily privileging a particular outlook over another, we discuss the main issues associated with these application-specific parameters, and the constraints they entail. More algorithm- or application- oriented taxonomic reviews are available elsewhere [14,180,224,117,32,138]. A brief account of relevant techniques accompanies the discussion of the issues. A detailed summary of each method or application would be beyond the scope of this chapter. Instead, we provide a generic description of the main algorithmic classes and more specifically discuss their interactions with the issues we have identified.

We begin with some reflections on the definition of segmentation. Section 3 then characterizes the input images from which organs and structures must be segmented, most especially in terms of dimensionality. We also introduce the commonly used radiological modalities referred to in this chapter, considering difficulties they create for segmentation techniques. The selection of an appropriate segmentation paradigm, which depends on the envisaged application and the imaging modality, is examined in Section 4. We analyze how the flexibility, locality and continuity of the model impact the segmentation performance. Section 5 discusses the introduction of *a priori* knowledge and medical expertise to guide the segmentation process towards more probable shapes. We then comment on the robustness of segmentation techniques in Section 6 where the difficult matters of initialization and the trade-off between genericity and application-specificity are emphasized. Validation is discussed in Section 7. We analyze its inherent contradictions (lack of true gold-standard due to inter/intra operator variability, conflicting error measures, application specificity) and how they bear on issues raised so far. Finally, Section 8 comments on the future of medical segmentation and the underexplored territories of semi-automated and manually-assisted segmentation.

## 2. Segmentation criteria

Biomedical images, being digital pictures, are organized collections of values linked via a chain of treatments and sensors to some underlying physical measures (radiation absorption, acoustic pressure, radiofrequency responses, etc.). These measures are related to the physical characteristics of the imaged tissues (density, chemical composition, cellular architecture). In that respect, these images are a means to analyze otherwise undecipherable raw measurements. The necessity to understand the measured values then becomes that of extracting meaningful information from the associated images, that is, to establish a relationship between the acquired data and the associated physiological phenomena. Segmentation is the first step on the path towards understanding these complex inter-relationships.

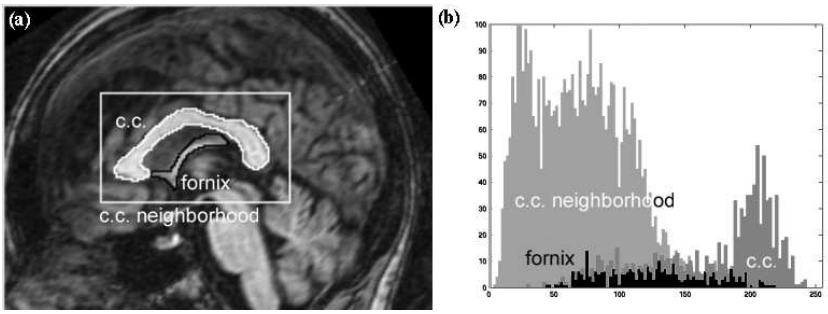


Fig. 2. The corpus callosum (c.c) and its neighbours in a T1-weighted MRI section (a) and their associated intensity distributions (b).

Irrespective of the envisioned application, segmentation essentially consists of partitioning the input image into a number of disjoint regions, so as to satisfy in each region a given criterion. This criterion may be derived from the intensity distribution of the underlying voxels in the image, or from the morphology of the region, among other choices.

The first difficulty in designing an adequate criterion is characterizing the objectives of the segmentation process, which may vary quite subtly from one application to the next and often depend on the object being segmented. For instance, the segmentation accuracy required to construct anatomical atlases (built by averaging the shapes of several segmented instances of the structures in the atlas) may be somewhat less than that required to quantify gray matter loss in a neurological study [172]. Indeed, missing the true boundary between gray and white matter might significantly bias the analysis in the latter case, whereas the errors introduced by the atlas shape averaging process are often as significant as those of a standard segmentation step. Therefore, even though correctly dealing at the criterion level with partial volume effect voxels (voxels to which multiple tissues contribute, which result in blurred edges at the surface of structures) may not be so crucial for atlas building, it is pivotal for accurate quantification of subtle tissue changes.

The second difficulty is linked to estimating the effects of noise and of the plethora of artifacts that plague the input images (bias fields, projection errors, variability in tracer uptake times, etc.). Together with more structure-specific parameters (contrast with respect to surrounding tissues, shape variability), these are bound to influence the choice of a segmentation criterion, most especially in terms of its leniency and permissiveness (and false positives and negatives).

In turn, the characteristics of the chosen criterion will affect the efficiency of the optimization or evolution process to which most segmentation applications can be reduced (see Section 6.3). Evaluating this efficiency (that is, assessing the performance of the segmentation system) is however particularly difficult in the absence of a satisfactory ground truth (we comment on this validation issue in Section 7).

### 2.1. *Hard segmentation*

From a mathematical point of view, image segmentation is an injective process that maps sets of voxels (low-level numerical bits of information) to annotated regions (high-level semantic information). These annotations may be actual labels (in reference to some dictionary of labels) or simply ordinal numbers to differentiate the regions.

More formally, let $I$ be an input image, defined by its value (usually a scalar intensity value, but sometimes a real-valued vector or even a tensor) at each point of its domain $\Omega$. Let $\omega$ be a non-empty subset of $\Omega$. Then let $\Lambda$ be a predicate (the above mentioned criterion restricted to a single target organ or structure) which assigns the value true or false to $\omega$. A segmentation of image $I$ for predicate $\Lambda$ is a partition of $\Omega$ into $n$ disjoint non-empty subsets $\{\omega_i\}_{i=1}^{n}$ such that:

- $\forall i,\, 1 \leq i \leq n,\, \Lambda(\omega_i) = \text{true}$; and
- $\forall i, j,\, 1 \leq i, j \leq n,\, i \neq j,\, \Lambda(\omega_i \cup \omega_j) = \text{false}$.

For example, in thresholding approaches (see Section 4.2.2), perhaps the simplest image segmentation approach, regions in $I$ are defined by creating a partition of the image intensities [160]. If we restrict $I$ to take values in $[0, 1]$, a choice for $\Lambda$ could be:

$$\begin{aligned} \Lambda : \Omega &\rightarrow \{\text{true, false}\} \\ \omega &\mapsto \begin{cases} \text{true if } \forall x \in \omega,\, I(x) > \theta \\ \text{false otherwise} \end{cases} \end{aligned}$$

where $\theta \in [0, 1]$ is a threshold, usually determined from the image intensity histogram (see Figure 2).

Note that $\Lambda$ often relies on a neighborhood of $\omega_i$ to assign it a boolean value (see Section 4.2): in other words, it is not a uniformity predicate.

### 2.2. *Soft segmentation*

Fuzzy segmentation [91] generalizes this predicate to a membership function, providing an efficient means to deal with partial volume effects,

Given a set of $K$ tissue or target classes $C = \{c_1, \ldots, c_K\}$, $K$ membership functions are designed: $\forall k \in [1, K]$, $\mu_k : \Omega \rightarrow [0, 1]$, subject to the constraint

$$\forall x \in \Omega,\, \sum_{k=1}^{K} \mu_k(x) = 1$$

They represent the contribution of each tissue (i.e. volume fraction) at every voxel in the input image.

A number of fuzzy clustering techniques have been developed to automate the computation of these membership functions [199]. In the context of brain tissue segmentation, these classes may represent gray matter, white matter or cerebrospinal fluid for example [137,76]. Probability densities can also be substituted for fuzzy

membership functions within a classical *a posteriori* maximization / expectation-maximization framework [212,97].

Yet, apart from probabilistic and fuzzy atlases [191,193] which directly use probability densities of tissue memberships, most clinical applications require the actual boundaries of the segmentation targets to be accurately determined. Consequently, suitable cut-off and thresholds have to be selected to turn soft segmentations into hard ones, a non-trivial problem in itself.

## 3. Input data

Each imaging modality comes with a specific set of characteristics (structural or functional measures, actual spatial and temporal resolution, effective field of view, signal to noise ratio, etc.) and sheds a different light on the studied pathology or organ. Ideally, segmentation algorithms should be fed images acquired from the full battery of existing modalities: MRIs to act as anatomical references, histologic sections for precise pathological tissue analysis, PET/SPECT or functional MRI data to reveal metabolic or functional relationships, etc. However, practical considerations beg for compromises to be found. Imaging resources may be unavailable (not only are radiological machines very expensive, but each acquisition is also costly), there may be potential health hazards linked to the invasiveness of data acquisition (x-ray CT or PET radiations must be used with caution, histology is a *post-mortem* analysis), etc. Often, the availability of a set of imaging modalities will determine the medical objectives which can be reasonably achieved. Conversely, the envisaged applications (or standard diagnostic protocols) condition the acquisition of appropriate modalities. In any case, segmentation systems have to be designed, or adapted, accordingly.

### 3.1. *Image characteristics*

Since biomedical images are located at the interface between physical measurements and human cognitive processes (namely, image interpretation and analysis), their characteristics are intimately linked to those of both the imaging equipment that acquired them and of the mathematical model that allows their algorithmical manipulation. These two sets of features are intricately related. For instance, while x-ray films are inherently continuous in space, segmentation systems manipulate them as a discrete set of pixels, once digitized. Conversely, most deformable model approaches (simplex meshes [51], medial representations [143], etc., see Section 4) operate on discrete input images, such as MRIs or CT scans, represented as continuous functions by using interpolation techniques, thereby achieving sub-voxel accuracy. Images can then be considered either as continuous functions observed at a continuous or discretized positions in space, or as a set of discrete intensity values organized on a regular or irregular lattice. They may also be treated as observations of a random vector (where each component is a random variable associated to a site in a

lattice) or even as the realization of a stochastic process (for Markov random field approaches).

As much a characteristic of the input images as one of the conceived applications, dimensionality (the dimension of the space in which the segmentation algorithm operates) may also significantly affect the choice, implementation and behavior of a segmentation system. For instance, in one of the corpus callosum statistical variability studies mentioned above [190], only the mid-sagittal sections of the input MRI's were selected for delineation, whereas Narr *et al.* [127] used 3 additional 1 mm thick slices on each side. Clearly, even if a fairly simple 2-D algorithm should be sufficient to automate the callosal segmentations in the first case, the segmentation of actual surfaces would be better handled in a true 3-D segmentation system in the second case: the callosal surface obtained would be smoother and more globally coherent than those resulting from concatenating of successively segmented 2-D sections.

Incidentally, while some modalities are inherently 3-D (MR for instance, even though images are acquired slice by slice), or inherently 2-D (histological slices), others are so only artificially. X-ray images for instance are 2-D projections of a 3-D object; conversely, CT scans are 3-D volumes reconstructed from a series of 2-D projections (see Fuchs *et al.* [61] for a review). Projections often make for more difficult segmentations as the target boundaries of structures may be substantially distorted and the contours of other organs may be intercepted by the projection and may pollute the image, further umpairing precise target localization. Furthermore, 3-D reconstruction induces many artifacts which may reduce the signal to noise ratio [60,69]. Note that 2-D segmentation techniques are sometimes applied to 3-D data, one 2-D slice at a time [7,101]. This could be for complexity reasons (real-time constraints, limited memory resources), algorithmic reasons (thresholding techniques, for instance, are not affected by the dimensionality of the data space as they do not rely on neighborhood considerations: only the intensity at the considered voxel is taken into account) or application-oriented reasons (the corpus callosum may be easier to segment in a series of coronal slices on each side of the mid-sagittal plane than in a 3-D MRI taken as a volume).

A hybrid dimensionality case, brain cortex parcellation deals with the segmentation of patches on 2-D surfaces folded in 3-D space (2-D manifolds) and often requires specialized segmentation systems [152,160,195] where the expected geometry and topology of the manifolds have to be woven into the contour-finding algorithms.

### 3.2. *Modalities*

We consider in this chapter only the most commonly used radiological modalities. Macovski [107] and Sprawls [174] provide in-depth introductions to the underlying physical phenomena.

Arguably the most common modality, radiography encodes in each voxel of the generated image the accumulated density of the structures intercepted by a beam of ionizing radiations (x-rays). This is a fast acquisition process which yields a particu-

larly high contrast between hard structures (such as bones) and soft tissues (organs). Unfortunately, radiography is also substantially invasive, suffers from the projection issues mentioned above (poor localization, decoy structures), and provides only limited information about soft tissues. In the related fluoroscopy, a contrast agents in injected into the patient and a moving x-ray beam enables the observation of structures in vivo and in real time. Among other applications, digital mammography has proved invaluable for the early detection of tumors and microcalcification clusters. In view of the poor contrast of structures in breast images, the robust detection of tumors is more important than the accuracy of their segmentation.

Another x-ray based modality, computed tomography (CT) alleviates most of the projection issues of planar radiography. It provides excellent soft tissue constrast and allows the 3-D visualisation of deep internal structures.

In ultrasound imaging, high frequency sound waves replace the ionizing radiations of radiographic techniques. The sound waves emitted by a transducer moved over the patient skin by an operator, are reflected back to the transducer at the interfaces between the traversed organs or tissues. An image of the variations of accoustic impendance can subsequantly be reconstructed. Ultrasound systems are completely non invasive, operate in real time and allow multi-planar imaging. Their low cost has ensured a wide dissemination. They can observe static organs and follow their dynamic evolution. They are however plagued with high level of speckling. Furthermore, bones and air act as opaque screens and prevent the visualization of deep structures.

The modality of choice for segmentation systems, magnetic resonance imaging (MRI) records the radio-frequency signal emitted by the protons of water molecules after excitation by a strong magnetic field. It provides excellent soft tissue contrast (most especially as it can be tuned by using an appropriate pulse sequence), high signal-to-noise ratio and good spatial resolution (commonly $1\text{mm}^3$) to the detriment of the temporal resolution, unfortunately (20 minutes for a standard examination). Besides, a number of intensity inhomogeneities and artifacts [169,171] complexify the segmentation task. A large number of dedicated overviews are available [224,32,14].

In scintigraphy, radioisotopes are injected into the patient and a series of cameras correlate the emitted beams to reconstruct a 3-D map of increased or decreased activity. It is an inherently functional modality, which unfortunately suffers from poor spatial resolution.

## 4. Segmentation paradigm

A segmentation paradigm encompasses under a single umbrella the many considerations about the nature of the segmentation application (statistical variability analysis, CAD, tumor tracking), the associated operational constraints, the algorithmic class of the selected segmentation technique and its working hypotheses, among others. As such, it depends on the envisioned application and on the imaging modality employed. For instance, segmentation of gray and white matter in a

cerebral MRI induces vastly different constraints from that of vertebrae in an x-ray of the vertebral column, in terms of target topology, prior knowledge, choice of target representation, signal to noise ratio, and dimensionality of the input data. The selection of an adequate segmentation paradigm is therefore pivotal as it affects how efficiently the segmentation system can deal with the target organ or structure, and conditions its accuracy and robustness. We detail below the foremost compromises and parameters that should shape an educated choice.

### 4.1. *Bottom-up versus top-down*

Reminiscent of the bipolar character of the couple image / application, segmentation involves extracting from the input image the relevant features (texture patches, edges, etc.) associated with the target structure and immersing these into a higher-order model of the target (surface mesh, m-rep, etc.). These are then passed to the application for analysis. Not surprisingly, this dual nature is reflected in the dichotomy between feature-extraction algorithms (bottom-up) and model-based approaches (top-down).

Bottom-up strategies can usually be decomposed into three stages: first, features are extracted, then they are grouped into several regions or contours, which, finally, serve to identify the structure's boundaries. However, since these techniques usually consider only local neighborhoods without a higher order comprehension of the nature of the image [a], they are prone to generating invalid outlines. For instance, in edge detection, all extracted contours do not correspond to the boundaries of the target structure: some of them may merely follow decoys or noise artifacts. These problems are rooted in the inherently numerical nature of the data manipulated by these low-level *model-free* algorithms, and aggravated by the underconstrained nature of the segmentation of highly variable structures. As such, image-level segmentation techniques (region growing, edge detection, etc.) tend to operate adequately only under substantial expert guidance.

On the other hand, high-level *model-based* approaches (top-down strategies) operate on semantic concepts (shape, appearance, relative position with respect to surrounding structures, etc.) associated with a representation of the actual segmentation target, extracted from the image. They are linked to the interpretation and understanding of the input data and can overcome many of these limitations [b].

[a] That is, they operate on values attached to the image voxels without necessarily establishing a relationship with the reality that they represent.

[b] Incidentally, whereas model-based approaches usually require a training set of segmented contours as an input, low-level feature extraction is generally performed without reference to an *a priori* contour model. Such distinction between the problem of contour modeling and that of edge extraction is characteristic of Marr's vision paradigm [114]. The interest of that dichotomy lies in its ability to decompose the segmentation problem into independent and manageable tasks. Unfortunately, it may also result in a unidirectional and somewhat irreversible cascade of errors. Furthermore, due to image noise and the image projection process, local model-free edge extraction is an ill-posed problem with no unique solution [145].

As such, top-down strategies provide a convenient framework to include *a priori* knowledge and medical expertise (see Section 5). Briefly, they also consist of three stages: model building (based on prior knowledge or on structures segmented *a priori*), model initialization (initialization of the parameters that control the model's shape, position, etc.), and model matching (adaptation of the parameters to the input image). By considering the target boundaries as a whole, they become a lot more robust to noise and imaging artifacts than bottom-up techniques. Unfortunately, they are also potentially less accurate. Indeed, the reference *a priori* models which act as shape, intensity, or distance constraints effectively prevent the segmentation of what they identify as noisy or invalid contours. When these correspond to actual noise, robustness is increased. However, when they correspond to the true contours of the target structure, accuracy decreases (Section 6 comments on this trade-off between accuracy and robustness, which also relates to locality, flexibility and continuity).

Often, a segmentation system will implement a mixture of bottom-up and top-down approaches, either explicitly [18] or implicitly (as with deformable models, see Section 4.3).

### 4.2. *Locality*

Locality refers to the extent of the neighborhoods around the voxels of the input image considered by the segmentation process. It is inherently linked to the segmentation strategy discussed above. Namely, very local techniques are usually considered bottom-up approaches (the size of the neighborhood being too small for an actual model to be used) whereas global techniques are ideally suited for introducing shape or appearance models. Local segmentation methods tend to be very fast, owing to the small number of parameters considered at each voxel [74]. In the absence of a model, they are more accurate (immune as they are from constraints linked to the geometrical arrangement of voxels or to their intensity distribution) but they are also more sensitive to noise and inhomogeneities. Conversely, larger neighborhoods increase noise robustness at the expense of accuracy.

In the absence of high-level models, local techniques are effectively a special case of classification algorithms. Segmentation then consists in deciding, for every voxel in the input image, whether or not it belongs to the target structures, based on attributes (intensity values, geometric descriptors or other statistics) collected in its immediate neighborhood.

On the other end of the locality spectrum, we find most of the model-based (top-down) approaches. These use the maximum amount of information that can be gathered from the underlying image to fit the parameters of the models they rely on and to guide the segmentation process (the considered neighborhood is then often extended to the voxels in the vicinity of the entire model surface, or even to the whole image).

After a generic description of voxel classification methods, we detail more specific local approaches in Section 4.2.2. The main global techniques, deformable models and atlas warping approaches are discussed later in sections 4.3 and 5.2.

#### 4.2.1. *The classification paradigm*

Classification techniques associate every voxel in the input image with a unique lable, or class, where classes are built from the voxel attributes [54] (usually, one class per segmentation target, plus a "non-target" class). In the simplest general case, voxels are classified independently of each other as the criteria employed, often based on distances between attribute vectors, do not take into account their geometric arrangements. As such, classification is really only a pre-processing step. Connected components must be extracted from the classification map to effectively segment the input image.

From a pattern recognition point of view, classification techniques aim to partition the multidimensional feature space formed by the voxel attributes. This could be a supervised or unsupervised process.

**Supervised classification.** Supervised methods consist of two phases: a training phase in which a learning set of *a priori* segmented structures help adjust the classifier parameters, and a classification phase where a previously unknown input image is processed with the trained classifier. A large number of supervised techniques are available in the literature (see Duda and Hart [54] for a review).

In view of the difficulty of modeling the probability distribution of the target voxel attributes, non-parametric techniques, which make no hypothesis about the class distributions, have proved popular. Nearest-neighbor classifiers for example assign a voxel to the same class as the voxel in the training set which is closest in terms of attribute distance (often, the class of the learning set voxel with the closest intensity). A generalization of this straightforward approach, a $k$-nearest-neighbor classifier [79] assigns classes based on a majority vote of the $k$ closest voxels in the learning set. Parzen window techniques extend the majority vote to a rectangular or spherical neighborhood of the attribute space centered on the considered voxel.

When the distribution of the attribute values is better behaved, parametric classifiers may increase the segmentation performances [54]. Often, voxel attributes are assumed to be drawn from a mixture of Gaussian distributions, as with the maximum likelihood classifier (Bayes method). Training such a classifier requires estimating the means and standard deviations of the Gaussian distributions and their mixing coefficients from the learning set of *a priori* segmented structures. In the classification phase, voxels are then assigned to the classes which maximize the posterior probability.

**Unsupervised classification.** When no *a priori* learning set is available to train the classifier, unsupervised classification (clustering) become a more suitable alternative. In the absence of an initial parameter fitting phase, clustering techniques often maintain, for each class, a model of the characteristics of their attribute distribution. These models are iteratively updated during the classification process, which usually alternates between classification and model fitting. The training phase is consequently distributed over the entire course of the classification phase.

The unsupervised version of the $k$-nearest-neighbor algorithm, the $k$-means clustering algorithm [87] models each class by its mean attribute vector and partitions the voxels in the input image by assigning them to the class whose mean is closest. By introducing fuzzy membership functions into the classification step, the fuzzy $c$-means algorithm [99] allows for a soft segmentation of the input image. A parametric unsupervised technique, the expectation-maximization algorithm (EM) assumes a Gaussian mixture model for the voxel attributes and iterates between the computation of the posterior probabilities associated to each class and the maximum likelihood estimation of the model parameters (means, covariances, mixing coefficients) [119]. Note that unsupervised techniques are often more sensitive to the initial values of their parameters than supervised classifiers [54].

**Feature selection** Often, the voxel intensity alone is considered as an attribute. However, when multiple attributes are available, an "optimal" subset of attributes, as discriminating as possible, must be selected while keeping the number of selected attributes reasonably small. This selection task (also called feature reduction) is a fundamental problem in statistical pattern recognition. Indeed, reducing the number of attributes saves computing resources by discarding irrelevant or redundant features. It also alleviates the effects of the so-called *curse of dimensionality* [83], which links the ratio: sample size (in the learning set) / dimensionality of the feature vector to the classification performances [c].

Given an objective function, which evaluates the performance of the classifier on an *a priori* set of measurements, the feature selection problem then boils down to a search problem in the combinatorial space defined by the voxel attributes. Trying out, in a brute force manner, every possible combination of features can be prohibitively costly when the number of attributes is high (although, as argued by Cover [43], traversing the entire search space is the necessary condition to an optimal selection). Specific sub-optimal selection strategies have therefore been suggested in the literature. They either rely on *a priori* knowledge about the classification problem at hand to discard features, or use generic optimization heuristics when

[c]Namely, when the dimensionality of the feature space increases, more parameters must be estimated, which enhances the risk of overfitting the model: adding new descriptors then usually first increases the classification performance, which attains a peak value, before decreasing as more descriptors are added (overfitting phenomena).

no domain-specific information is available (or when it is too difficult to exploit). Algorithms as diverse as stochastic annealing, genetic algorithms, max-min pruning, principal component analysis or neural network node pruning have been introduced (see Jain *et al* [84] for a taxonomy of feature selection algorithms).

**Applications.** In view of the tremendous shape and topological variability of the human cortex, brain tissue segmentation in MRI is a natural application for classification techniques [102]. The many intensity inhomogeneities and bias fields mentioned in Section 3.2 tend to favor unsupervised clustering approaches [103,71,137,158] even though *a priori* intensity models of the cerebral tissues may also prove adequate [212,23]. However, due to its highly convoluted morphology, the gray matter ribbon comprises a large proportion of partial volume effect voxels in typical T1-weighted MRIs. There are often better handled by fuzzy approaches [30,156]. Classifiers are also ideally suited to extract lesions and tumors in digital mammography [150] or in MRI [31], using a combination of intensity and texture attributes.

#### 4.2.2. *A few classification approaches*

We detail in this section three commonly used classification techniques in decreasing order of locality (thresholding, region growing and Markov random fields) and briefly comment on more exotic classification techniques at the end.

**Thresholding.** As far "left" as could be on the locality spectrum, thresholding algorithms (see Sankur *et al.* [163], Sahoo *et al.* [160] or Lee *et al.* [96] for broad overviews) do not consider any neighborhood in the image *per se*: the classification is based solely on comparing the voxel's intensity and an intensity threshold that is set in advance, or determined globally from the intensity histogram of the input image. A partition of the input image is therefore obtained by partitioning the image intensities. When the histogram is multi-modal, several thresholds can be computed. As could be expected from a local technique, the effectiveness of a thresholding algorithm depends on the contrast between the target structure or tissue and the surrounding ones. Several improvements have been made to increase the segmentation robustness. In Lee et al. [95] for instance, connectivity constraints were added to separate regions that would otherwise be incorrectly merged. A number of local histogram thresholding techniques are also available (iterative Bayesian classification [113], dynamic thresholding [126], etc.).

Thresholding techniques have been mostly applied to the segmentation of digital mammograms, either as a first-stage segmentation tool to provide a second-stage classifier with candidate pathologies [147,81], or to determine with enhanced accuracy the location of masses in previously pathologically labeled images [70]. Highly contrasted structures such as bones in CT [227,68] or the cavities of the left ventricle in cardiac MR [50,170] can also readily be segmented by thresholding techniques. In Zimmerand *et al.* [226], ovarian cysts were extracted from ultrasound images with an

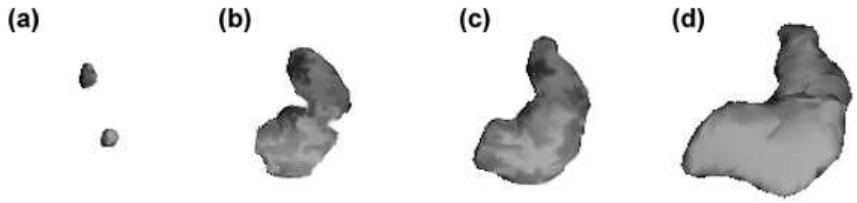


Fig. 3. Four steps of the region growing segmentation of a human hippocampus from a $1mm^3$ T1-weighted MRI of the head.

attribute vector consisting of intensity and texture descriptors.

**Region growing.** The simplest form of neighborhood information is exploited by region growing approaches that rely on the hypotheses that adjacent pixels have similar characteristics, and in particular, comparable intensity values. Region growing is then an iterative process that produces connected regions. First, a number of seeds are selected in the input image to form single voxel regions. Then, at each iteration, the neighboring voxels of those in the regions are tested against a similarity criterion and those that pass the test are added to the corresponding region. This process is repeated until no more voxels can be added or until a stopping condition is satisfied. Among the many similarity criteria, usually based on features computed on the regions, we find geometric ones (convexity, size, shape of region) and radiometric ones (intensity, texture) [73]. However, the fundamental assumption of feature consistency makes region growing techniques very sensitive to noise and imaging artifacts. Homotopic region growing techniques [111] have been developed to constrain the shape of the regions in the face of the potential topological changes (holes, fusion of previously disconnected regions, etc.) induced by imaging inhomogeneities. Furthermore, the placement of the initial seeds is particularly difficult to automate (although seed-invariant approaches are available [207]) and depends on the segmentation application (see Section 6.2).

In view of its many drawbacks, region growing, like thresholding techniques, often require post-processing. Its main applications are segmenting tumors and lesions in digital mammography [92,66] or in MRI [146]. Figure 3 shows four steps of the segmentation of a human hippocampus with a heavily regularized region growing algorithm initialized with two seeds.

**Markov Random Fields.** A favored means to model images in the presence of noise and artifact [75], Markov random fields (MRF) are particularly well-suited to capturing local intensity and textural characteristics of images as they provide a consistent way to model context-dependent entities such as image voxels and correlated features [9,49]. They rely on the assumption that the intensity of any given

voxel partially dependent on those of its neighbors (that is, that neighbor voxels belong to the same class, or that they must belong to an *a priori* defined class, e.g. voxels from the amygdala class are not allowed to be posterior to voxels from the hippocampus class). In the context of medical image segmentation, the hypothesis becomes that of a low probability for a single voxel of a given class to occur inside an homogeneous group of voxels from another class.

A defining characteristic of an MRF system is the shape and size of the neighborhood system imposed on the voxels of the input image. Inside these neighborhoods, cliques (subset of sites in which every pair of distinct sites are neighbors) are often used to define the conditional MRF distributions that characterize the mutual influences between pixels and textures.

In accordance with the Hammersley-Clifford theorem [13], an MRF can also be represented by a Gibbs distribution

$$P(x) = Z^{-1}e^{-U(x)}$$

where $Z = \sum_{x \in X} e^{-U(x)}$ is the so-called partition function that acts as a normalizing constant, and $U(x)$ is the associated energy function, which is usually much easier to manipulate.

In this framework, segmentation consists of estimating a label process $\Lambda$ from the realization of a voxel process $\Pi$. Rather than directly modeling $P(\Lambda = \lambda | \Pi = p)$, a Bayesian approach is generally used to compute the conditional probability from a fixed probability law imposed on $\Lambda$ and an estimation of $P(\Pi = p | \Lambda = \lambda)$. $\lambda$ can then be iteratively approximated by maximizing this *a posteriori* probability, which boils down to minimizing the compound energy $U$ associated with the MRF model. Among the many optimization approaches, we find iterated conditional modes [13] and stochastic simulated annealing [64].

In spite of their high computational demands, MRF techniques have been successfully applied to a variety of medical image segmentation tasks. Their ability to handle local inhomogeneities and topologically complex voxel arrangements makes them ideally suited for brain tissue segmentation in MRI [75,153]. Other MRI applications include knee image labeling [28], cortical sulci [159] and magnetic resonance angiograms segmentation [200]. MRF texture models have proved useful in the segmentation of lung in chest radiographs [205], bones in CT [135] and, of course, pathological masses in digital mammography [26,101,57].

**Exotic classifiers.** In addition to the above mentioned techniques, less standard classification approaches are also available [54]. Neural network in particular are worth detailing.

Artificial neural networks (ANN) are mathematical tools that mimic the densely interconnected and parallel structure of the brain, and the adaptive biological processes of the nervous system, both in terms of learning and of information processing. They are composed of a large number of processing elements (so-called neurons)

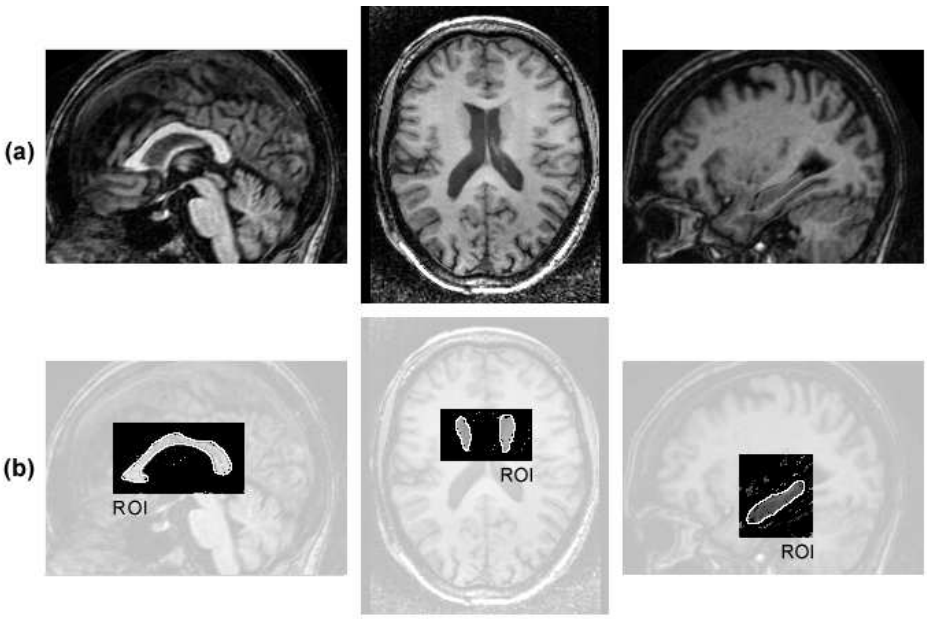


Fig. 4. Neural classification of corpus callosum, caudate nucleus and hippocampus: (a) input MRI; (b) extracted structures (after thresholding of classification map) with true outlines superimposed. The classifier was trained and applied only to the unshaded regions of interests (ROI).

linked together by weighted connections (analogous to synapses). Each neuron receives activation signals from other neurons and outputs a non-linear function of the weighted sum of these activations. This nonlinear mapping function ($\phi$) is called the activation function. A commonly used activation function is the sigmoid function (hyperbolic tangent for instance). Output from a neuron $neuron_i$ is then written:

$$neuron_i\left(x\right) = \phi\left(w_i^t x\right) + w_{i,0}$$

where $x$ is the $d_i$ dimensional vector of input signals, $w_i$ is the weight vector (or vector of synaptic weights), and $w_{i,0}$ is a constant bias.

A neural network is then a graph of interconnected neurons, whose connectivity matrix defines the connection pattern. Given a learning set of labeled samples, training an ANN then essentially consists of modifying the weights of its neurons so as to minimize the overall difference between the output values of the network and the target values from the learning set. The most popular learning technique is the so-called back-propagation algorithm, which is based on a straight-forward gradient descent technique. Various more sophisticated learning techniques have been developed, please refer to [214] for a broad overview.

Neural networks have been mostly used to segment tissues and structures in MR images [14,155,216,208]. Hall *et al.* [71] also used them to segment tumors and edema. They can also be employed as a pre-processing stage for other segmentation algo-

rithms [204,140,56]. Figure 4 displays the classification results for three cortical structures (corpus callosum, caudate nuclei and hippocampus) obtained with the two stage neural network presented in Pitiot *et al.* [139].

### 4.3. *Flexibility*

In this chapter, flexibility stands for (1) the actual geometrical and topological flexibility of the segmentation process and of the underlying shape or intensity models if available, as well as (2) their combined expressivity, that is, their ability to represent a variety of shapes and appearances with a minimal number of parameters. Because of their high accuracy, local techniques (classification approaches in particular) are geometrically and topologically very flexible. Clearly, their locality enables them to segment arbitrarily complex arrangements of voxels. However, they are not compact in that they often require as many parameters as there are voxels in the input image to represent the extracted structure or tissue.

We submit that the use of a segmentation model is a necessary condition to achieve true flexibility. We therefore focus our discussion of this issue on deformable models, and in particular on how they are formulated: explicitly or implicitly.

Deformable models [117] are model-based (top-down) segmentation approaches that evolve parametric surfaces or curves in fashions inspired by mechanics and physics [d]. They are characterized both by their surface representation (continuous or discrete, explicit or implicit) and by their evolution law, which determines the space of available shapes (see Montagnat *et al.* [123] for a thorough taxonomy). Once initialized reasonably close to the segmentation target (in terms of position and of shape), they often deform via iterative relaxation of a compound functional $E$. Classically, $E$ is made up of three terms:

- an internal (or regularization) energy $E_{internal}$ which characterizes the possible deformations of the deformable surface,
- an image coupling energy $E_{image}$ which couples the model to the image, and
- a constraint energy $E_{constraint}$ which regroups the various available constraints (shape, appearance, etc.).

We get:

$$E = \alpha.E_{internal} + \beta.E_{image} + \gamma.E_{constraint}$$

with $\alpha$, $\beta$, $\gamma \in \mathbb{R}$.

Typically, the internal energy measures the amount of bending and stretching undergone by the deformable model as it evolves. A large number of image forces

[d] As the name indicates, deformable models generally behave like elastic bodies, within a Lagrangian dynamics framework.

are also available [124]. They can be based on the gradient of the input image [123], on a smoothed version of its associated edge-image [142], on intensity profiles [27], etc.

Alternatively, the evolution of the deformable model can be controlled by a dynamic equation within a Lagrangian framework (following the reasoning detailed in Section 6.3), or within a Bayesian probabilistic framework [117].

When the deformable surface is described by coordinate functions that depend on a vector of shape parameters, the model is explicit. Alternatively, implicit formulations model the surface with implicit equation. At a glance, explicit parametric models are the most frugal in terms of parameters, while implicit models, level sets or atlas registration (see Section 5.2), win the palm of flexibility.

Explicit parametric models are especially interesting in medical image segmentation for the following reasons. First, as detailed below, they can adequately handle the various discontinuities that sampling artifacts and noise create on the boundaries of the target structures. Also, they compactly describe a wide variety of shapes while minimizing the overall number of parameters or masking these behind a small and easily manageable set of physical principles. They often provide a local, if not global, analytical model of the structure once segmented, which makes it easier to analyze subsequently. Finally, *a priori* knowledge about the shape, location, or appearance of the target structure can guide the deformation process: deformable models are then the framework of choice to mix bottom-up constraints computed from the input images with *a priori* top-down medical knowledge.

Inspite of these advantages, explicit models raise several practical concerns, most of which are linked to the somewhat delicate balance between the contributions of the internal and external forces or energies. Clearly, as image coupling forces may drive the models towards the wrong boundaries (especially in the absence of prior knowledge constraints), the regularization constraints must limit the geometrical flexibility of the models. The extent of this limitation is not trivial to determine *a priori*, and will often depends on the variability of the segmentation target and on the input image characteristics. As a result, explicit models often exhibit significant difficulties in reaching into concave boundaries. Balloon forces [35], gradient vector flow [217] or dynamic structural changes (subdivision of model basis functions [122], densification of control points in regions which undergo dramatic shape changes [201] or which are too far from the closest potential boundary [142]) are a few of the many techniques developed to control the accuracy of the segmentation scheme and address this restriction. Furthermore, most models cannot accommodate topological changes since these are usually not coded into the model parameters. Still, a few topologically flexible approaches are available in the literature that can adapt the topology of the deformable surface as it evolves [164,215,109,201,118,52]. Finally, they are also notoriously sensitive to initialization (we tackle this particular issue in Section 6.2).

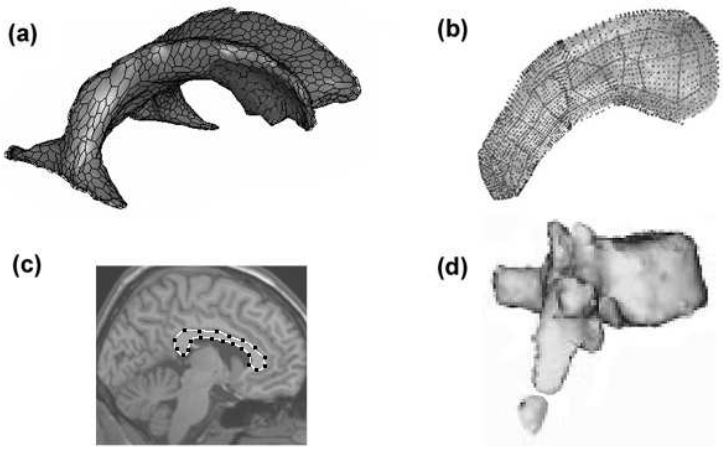


Fig. 5. Four types of deformable models: (a) simplex mesh of ventricles; (b) m-rep of hippocampus (courtesy of Pizer *et al.*); (c) B-spline representation of the mid-sagittal slice of the corpus callosum; (d) level-set of vertebra (courtesy of Leventon *et al*).

A popular implicit formulation, level sets model deformable surfaces [180] using a higher dimensional signed function whose zero level corresponds to the actual surface. From the desired properties of the surface evolution process, an adequate flow equation can be derived for the embedding signed function.

Initially proposed by Sethian and Osher [130,167] to track moving interfaces in fluid mechanics and combustion simulations, level sets alleviate both the parameter granularity issue of explicit approaches (namely, which sampling strategy to choose to parameterize the deformable surface) and their difficulties in handling topological changes. Their main drawbacks are linked to their inherently implicit formulation, which makes it difficult to analyze the segmented surface, once extracted from the input image, in the form of an unstructured set of voxels. It also makes it substantially awkward to incorporate prior medical expertise into them. Finally, like explicit models, they are quite sensitive to initialization. Other implicit formulations include algebraic surfaces [184], superquadrics [10] and hyperquadrics [34]

Not surprisingly, deformable models (explicit and implicit) have been mostly applied to the segmentation and tracking of anatomical structures.

Aside from the cerebral cortex [45,63] and the ventricles [168], they have been widely employed in the segmentation of most of the deep gray cortical structures (corpus callosum [140,202], hippocampus [144,202], caudate nuclei [168,140], etc.). A natural segmentation target in x-ray images, the extraction of bones has also proved amenable to the use of deformable surfaces [134,186,220]. Soft tissue organs such as the liver [125,62], the kidney [86], the stomach [110] or the heart [25,165,118] have also been targeted.

Because of their dynamic nature, deformable models have been immensely pop-

ular in motion tracking applications, most especially in ultrasound images [108,121]. Finally, they have also been applied to the delineation of a variety of lesions and tumors: brain tumors in MRI [77], cysts in ultrasound breast images [219], etc. Please refer to McInerney *et al.* [117] for additional applications and Figure 5 for an illustration.

### 4.4. *Continuity*

In view of the various irregularities that sampling artifacts or noise induce along the target contours in the input image, boundary continuity is another constraint that substantially affects the analysis of the segmented target. For instance, statistically comparing the shape variability of anatomical structures across diseased populations or between normal subjects and disease groups [127], or computing an average pattern of gray matter growth across a population of patients [172], is much more easily and accurately performed when continuous surfaces (discrete meshes in these cases) are used to represent the target tissues or structures instead of the unstructured and quite probably topologically complex sets of voxels that level set techniques would produce [e]. This allows noisy and possibly sparse local image features to be structurally linked inside a coherent and compact model.

Use of a continuous segmentation model (deformable models, for instance) in conjunction with a continuous representation of the image space (via interpolation techniques [98]) also enables sub-voxel accuracy. This is especially interesting when the radius of the target structure is not large with respect to the resolution of the input image (for example, for the segmentation of small lesions in MRI, or of organs in standard 2x2x4mm PET scans). The segmentation results are however particularly difficult to validate in this case as little to no information is available to compare, inside each voxel, the location of the segmented contours to those of the actual structures.

On the other hand, continuity can be a hindrance to accurate segmentation. For instance, the quantification of cortical gray matter loss in Alzheimer disease[188] does not require that voxels classified as gray matter form a single connected component. Ensuring the extraction of the cortical gray layer by a single continuous surface or by a single voxel connected component would only prevent difficult to reach regions from being segmented. As an illustration, the inferior horns of the human brain ventricles are connected to the rest of the lateral ventricles via a group of partial volume voxels that are exceedingly difficult to segment in standard T1-weighted $1mm^3$ resolution MRIs (to the point where a lot of manual delineation protocols will just exclude them for fear of introducing an artificially high shape variability). Consequently, a region growing approach initialized with seeds inside the main body

[e]Note that, as demonstrated in Leventon et al. [100] or Golland *et al.* [67], average anatomical shapes can still be computed from level set representations by averaging their associated distance maps. However, this approach makes the strong assumption, that pixels at the same location across the set of level set segmentation are homologous which certainly does not hold when topological changes occur, even when relaxed by the influence of the diffusion factor of the distance computation.

of the ventricles only would most probably stop at the PVE voxels and discard the inferior horns altogether. Likewise for deformable model techniques, the image coupling energy, often linked to the image gradient, would most likely prevent the model from reaching as far as the inferior horns. Clearly, this difficulty would not impede other classification techniques even though these might incorrectly exclude some of the PVE voxels. Similar considerations apply to the segmentation of the tail of the caudate nucleus in brain MRI (figure 7).

### 4.5. *Surface versus volume*

Aside maybe from the cortical gray matter layer which can be handled as a surface in typical $1\text{mm}^3$ resolution brain MRIs, most segmentation targets correspond to actual anatomical volumes, and behave like deformable solids. When the target boundaries have to be extracted from a single static image though, choosing between a surface or a volume representation is arguably a mere matter of taste since most of the features of volume segmentation systems useful on static images have their counterparts in surface segmentation systems and vice versa. However, in dynamic segmentation cases (organ tracking, for instance) much can be gained by using a volumetric framework within which physiologically or anatomically motivated constraints between structures or tissues are more easily incorporated.

Volumetric approaches are especially interesting in cardiac motion tracking applications [136,166,117] as they can model the thick-walled left ventricles as a whole instead of requiring difficult to synchronize endocardial and an epicardial surface models [1].

For these dynamic segmentation problems (which are often functional in nature), volumetric biomechanical models [116,132] could help increase the overall robustness, owing to their ability to encode the dynamics of the shape, appearances and relative positions of structures in an anatomically accurate and mechanically plausible way.

Undoubtedly, the choice of a surface or volume representation is in part dictated by how easily the extracted segmentation target can be analyzed in the envisaged application (average shapes are more easily computed on sets of surfaces than volumes, tissue loss is often simpler to assess from sets of voxels, etc.) and in part determined by the characteristics of the target itself embedded inside the input image (volumetric frameworks have typically proved more efficient than dual surface approaches in preventing thick walls from collapsing in the presence of heavy noise).

## 5. Expert knowledge (*a priori* information)

However variable in shape and appearance the target structures or tissues may be, their general morphology, contrast and relative position with respect to surrounding tissues and neighborhood structures is often known. In view of the many intensity inhomogeneities and the plethora of artifacts and decoys present in the input image, this *a priori* medical knowledge is an invaluable tool in the search for the best

trade-off between accuracy and robustness. In addition to facilitating the actual segmentation process, shape, appearance and position models can also significantly assist the subsequent analysis of the segmented target. Clearly, compact models are more easily interpreted and compared (between themselves or against statistically built average models and modes of variation) than tediously long lists of vertices or voxels.

The available corpus of medical information can be leveraged in essentially two ways: implicitly (computationally) and explicitly. Given a learning set of *a priori* segmented instances of the segmentation target, implicit knowledge algorithms have to automatically discover the relationships and functional dependencies of the various parameters of the model. However, explicit information about the target is often available, in the form of medical expertise. For instance, the relative positions of most of the deep gray nuclei in the bain is fairly consistant across individuals, anatomical structures do not usually intersect, etc. From these observations, a series of rules can be derived to better drive the segmentation process. Broadly speaking, explicit knowledge approaches can be seen as a special case of implicit knowledge algorithms where the additional medical expertise provides short cuts in the search for the target structure or tissue.

As mentioned earlier, model-based (top-down) methods are more amenable to the introduction of medical knowledge. Nonetheless, bottom-up techniques such as thresholding and region growing can also benefit from intensity models built from *a priori* observations.

We review below a selection of approaches organized according to the type of knowledge that they model: shape and appearance in Section 5.1 and position in Section 5.2. In each case, we propose a number of implicit and explicit knowledge techniques.

### 5.1. *Modeling shape and appearance*

#### 5.1.1. *Implicit models*

Even though a given structure can present a wide variety of forms, the notion of biological shape seems reasonably well explained by a statistical description over a large population of instances. Consequently, statistical approaches have attracted considerable attention [41,40,175]. A deformable model is then constrained not only by the number of degrees of freedom imposed by its geometric representation, but also in that it must be a valid instance of the shape model. Developed by Cootes and Taylor [41], active shape models are represented by both a set of boundary/landmark points and a series of relationships established between these points from the different instances of the training set. New shapes are modeled by combining in a linear fashion the eigenvectors of the variations from the mean shape [198]. These eigenvectors encode the modes of variation of the shape, and define the characteristic pattern of a shape class. The shape parameter space serves as a means to enforce limits and constraints on the admissible shapes, and insure that the final extracted

shape presents some similarity with the shape class, as established from the training set. Many variants have been presented in the literature [209,80]. They either introduce more constraints or decrease the control over admissible shapes. In particular, active appearance models [40] incorporate both a statistical model of the shape of the target, and a description of the statistical distribution of the gray-level intensities of the structure. A similar PCA approach was applied to the signed functions embedding level set representations in Leventon *et al.* [100].

Blum *et al.*[17] introduced the medial representation as a model of biological growth and a natural geometry for biological shapes. Pizer *et al.* [143] derived a sampled medial model. Joshi *et al.* [86] used it within a Bayesian framework to incorporate prior knowledge of anatomical variations. A multi-scale medial representation was used to build the template examples needed to obtain prior information about the geometry and shape of the target anatomical structure. Within this framework, the anatomical variability of a structure corresponds to the distribution of the admissible transformations of the shape model. Medial representations are however difficult to build for non symmetrical shapes and are notoriously plagued by topological difficulties.

Staib *et al.* [175] used a similar Bayesian scheme to control the coefficients of an elliptic Fourier decomposition of the boundary of a deformable template. They introduced a likelihood functional, which encoded the spatial probability distribution of each model, to be maximized under a Bayesian framework. The distribution of the model parameters was derived from a learning set of instances of the target object, and served to constrain the deformable template towards the most likely shapes. Székely *et al.* [182] added an elastic property to a Fourier decomposition to create elastically deformable Fourier surface models. A mean shape and its associated modes of variation were extracted via statistical analysis of a learning set of Fourier decomposed instances of the target structure. The elastic fit of the mean model in the shape space was used as a regularization constraint.

Styner *et al.* [179] combined a fine-scale spherical harmonics boundary description with a coarse-scale sampled medial description. The SPHARM description, introduced by Brechbühler [20] is a global, fine scale parameterized description which represents shapes of *spherical* topology. It uses spherical harmonics as a basis function. Styner's medial models were computed automatically from a predefined shape space using pruned 3-D Voronoï skeletons to determine the stable medial branching topology.

Metaxas *et al.* [120] devised deformable superquadrics which combined the global shape parameters of a conventional superellipsoid with the local degrees of freedom of a membrane spline. The relatively small number of parameters of the superellipsoid captured the overall shape of the target structure while the local spline component allowed flexible shape deformation in a Lagrangian dynamics formulation. Vemuri *et al.* [203] used the properties of an orthonormal wavelet basis to formulate a deformable superquadric model with the ability to continuously transform from

local to global shape deformations. Such model can continuously span a large range of possible deformations: from highly constrained with very few parameters, to underconstrained with a variable degree of freedom. Here again, a Bayesian framework biased the deformable models towards a range of admissible shapes.

Poupon *et al.* [149] proposed the use of 3-D moment invariants as a way to embed shape distributions into deformable templates. They devised a framework capable of dealing with several simultaneously deforming templates, thanks to their fairly low updating cost, with the goal of segmenting deep grey nuclei in 3-D MRI. The remarkable stability of the invariant moments allowed them to study the anatomical variability of the deep gray nucleir in brain MRI.

A given instance of the target structure may not always exhibit homogeneous intensity distribution along its boundaries. Yet, the intensity may be locally characteristic. The intensity profile, computed along the border of the structure models, then provides an efficient means to introduce *a priori* knowledge. Cootes *et al.* [39], for instance, modeled the statistical distribution of the intensity profile on each side of the structure surface. The mean profile, established from a structure learning set, was compared against the image data to determine the cost of a particular configuration of the model and guide the segmentation process. Brejl *et al.* [21] used a somewhat similar border appearance model to automatically design cost functions that served as a basis for the segmentation criteria of edge-based segmentation methods.

Note that most of these statistical or bayesian approaches require that correspondences between the shapes in the learning set be available *a priori*, a non-trivial problem in itself [196,33,59,209,89,192,46,48,141].

### 5.1.2. *Explicit models*

An even larger variety of explicit knowledge techniques is available in the literature. These approaches tend to be more heterogeneous as they usually combine shape and intensity descriptions in the same framework. Often, explicit information is complemented or generalized by implicit information (for instance, a purely explicit position rule can be made more robust as a fuzzy condition, which however introduces non-explicit elements: the $\alpha$ parameter of the cut-off, the amount of diffusion, etc.).

Since the seminal work on spring loaded templates by Fischler *et al.* [58], many explicit knowledge approaches have been proposed in the literature to incorporate computationally extracted medical expertise about the shape or appearance of a structure.

Early work frequently relied on highly specific hand-crafted models. Yuille *et al.* [221] chose to use circles and parabola to retrieve eye and mouth patterns in face pictures. Noticing the elliptical shape of the vertebra in axial cross section images

of the spine, Lipson *et al.* [104] used deformable ellipsoidal templates to extract their contours. These methods present the advantage of providing a very economical description of the shape in terms of the number of required parameters but lack genericity in that a new model with new parameters has to be developed with each new object.

Even though ASM can handle disconnected shapes it is easier to partition a complex shape (i.e. the vertebral column), into simpler and more manageable elements (the vertebrae). Nothing this, Bernard *et al.* [12] devised a two-level hierarchical scheme to model both the shape and the topology of the resulting complex model. Each individual structure was controlled by its own ASM, subject to an overall global ASM encoding the relative positions and orientations of the set of components.

Amit and Kong [3] used a complex graph of landmarks, automatically chosen from the input images as a topological model, to guide the registration process of x-ray images of the hand. A dynamic programming algorithm was used on decomposable subgraphs of the template graph to find the optimal match to a subset of the candidate points.

As it can represent and merge uncertain or imprecise statements, fuzzy theory is particularly well-suited to model shape. Among others, Chang *et al.* developed a fuzzy-controlled rule-based system capable of segmenting MR images of diseased human brains into physiologically and pathologically meaningful regions by incorporating expert knowledge about both brain structures and lesions. They used the distance between pixels and the ventricular boundary as a fuzzy property of periventricular hyperintensities to help diagnose the studied disease. Barra and Boiré [11] used information fusion to combine medical expertise with fuzzy maps of morphological, topological, and tissue constitution data to segment anatomical structures in brain MRIs. For instance, they encoded expert information about the relative position of two structures as a fuzzy distance map. Wen *et al.* [213] used fuzzy-embedded human expert knowledge to evaluate the confidence level of two matching points using their multiple local image properties such as gradient direction and curvature. Studholme *et al.* [177] merged region labeling information with classic iconic image registration algorithm via information fusion to align MR and PET images of the pelvis.

When anatomic knowledge can be captured by a series of simple positional, geometric or intensity rules, expert systems provide a convenient framework to assist in segmentation tasks. Ardizzone [5] for instance developed a descriptive language to express the geometric features and spatial relationships among areas of images. [115] also used a rule-based system to organize and classify features (such as brightness, area, neighborhood, etc.) for regions that had been automatically extracted via region growing and they segmented scalp, gray and white matter, CSF and strokes. In Brown *et al.* [22], lung boundaries were segmented in chest X-ray images by matching an anatomical model to the image edges using parametric features

guided by a series of rules. Li *et al.* [101] described a knowledge-based image interpretation system to segment and label a series of 2-D brain X-ray CT-scans. Their model contained both analogical and propositional knowledge on the brain structures, which helped interpret the image primitive information produced by different low-level vision techniques. Finally, Poupon *et al.* [149] used 3-D moment invariants to embed shape distributions in deformable templates. They devised a framework that could deal with several simultaneously deforming templates, with a fairly low updating cost, to segment deep gray nuclei in 3-D MRI. We presented in Pitiot *et al.* [140] an expert-knowledge guided system which evolved, in parallel, a number of deformable models (one per target structure). These evolutions were supervised by a series of rules and meta-rules derived from *a priori* analysis of the model's dynamics and from medical experience. The templates were also constrained by knowledge on the expected textural and shape properties of the target structures (caudate nuclei, ventricles, corpus callosum and hippocampus in T1-weighted MRIs).

## 5.2. *Position*

Often, the positions (and shapes) of nearby anatomical structures are not independent of each other. For instance in the human brain, the caudate nuclei are juxtaposed to the lateral ventricles, so any change in the shape or position of one will affect the other. Information about the respective position of structures can then dramatically help the segmentation process. Positional knowledge can be either relative (with respect to neighborhood structures) or absolute (with respect to an anatomical atlas or standardized coordinate system).

### 5.2.1. *Distance constraints*

Relative positional knowledge often takes the form of distance constraints. In Barra and Boiré [11] for instance, fuzzy logic was used to express both distance and positional relationships between structures. In Tsai *et al.* [197], a series of parametric models, built via principal component analysis of multiple signed distance functions, enabled the concurrent segmentation of anatomical structures, via minimization of a mutual information criterion. Inter-object distance constraints were also used in Yang *et al.* [218] where a maximum *a posteriori* estimator for anatomical shapes helped constrain the evolution of level set functions.

In Pitiot *et al.* [140], we also chose distance maps as they can model distance constraints accuratly and robustly (guaranteeing non-intersection, for instance). Given a deformable model $\Pi^0$ (a simplex mesh [51]), we wished to impose on it a distance constraint with respect to another model $\Pi^1$. We first computed the distance map $D^1$ associated with a discrete sampling of $\Pi^1$. We used a classical Chamfer map [19] algorithm to compute a signed distance map, positive outside the discrete sampling of $\Pi^1$ and negative inside. At each vertex $P_i^0$ of $\Pi^0$, we then computed a "distance force" $f_{distance}$ whose magnitude depended on the value of the distance map at the

considered vertex. We derived two types of constraints. For some pairs of structures, we wanted the force to attract the vertex, along the direction of the gradient of the distance map, up to an exact distance $d_{target}$ of the target mesh: For other pairs, we only wished to enforce that this same vertex remained at distance greater than $d_{target}$ (to prevent intersections between structures for instance). Note that these forces could also be applied to a subset of the mesh vertices (so-called "zones") to enforce more local constraints.

### 5.2.2. *Atlas warping*

A hybrid shape/position explicit knowledge approach, atlas registration or warping [183,8,36] enables the concurrent segmentation and labeling of several target structures. Prior anatomical expertise about the shape, orientation and position of the target structure is projected onto a 3-D atlas, usually modeled as an elastically (or fluidly) deformable object, to be used as anatomical reference. Segmenting the target structures then boils down to registering the *a priori* labeled atlas to the input image. In effect, this transforms a model-to-region matching problem (the initial segmentation task) into an intensity to intensity matching one (iconic registration of two images). As a result, the effectiveness of the process relies on the assumption that the actual target structures in the input image are only marginally different in shape, orientation and location from the ones in the atlas, a reasonable hypothesis in non pathological cases.

Atlas techniques usually consists of two phases. First, the atlas is initialized over the input image with a rigid or affine registration algorithm [4,93]. Then, a non-linear registration stage corrects for the finer anatomical differences [36,162,44,29]. Not surprisingly, the main drawbacks of this approach are classical registration issues. To begin with, a poor linear initialization will undoubtedly yield an even worse non-linear registration. Second, because of their tessellated nature, biomedical images are packed with decoy structures which look surprisingly close to the target ones and may fool the registration process. Finally, because of the high variability of the segmentation targets, the non-linear registration process may not be flexible enough to adapt the atlas contours to the convoluted boundaries of the actual structures, all the more since the regularization parameters of the non-linear registration have to be kept fairly high to prevent warping to incorrect boundaries and to avoid producing self-intersecting boundaries. One way to alleviate this issue is to restrict atlas registration to only the initialization step of the segmentation process (see Section 6.2). Another work-around consists in using preprocessing techniques. In [161] for instance, 3-D edge detection and a series of morphological operators were used to extract from the input MR images the main cortical sulci. These helped increase the convergence speed of the atlas warping procedure by providing a smooth representation of the cortical surface.

Atlas warping has been mostly applied to the segmentation of cerebral struc-

tures in MR images of the brain [194]. Aside from the segmentation *per se*, it also provides a standard reference space in which to study the morphometric properties of structures and organs [47,85].

## 6. Robustness

A segmentation system can arguably never be robust enough, as exemplified by the variety of techniques discussed in the literature to cope both with the high variability of the target structures and with the noise characteristics of the input images. However, as already mentioned above, increased robustness often comes at a cost, that of decreased accuracy. As always, trade-offs have to be found, which we discuss in this section, along with the two main robustness factors: initialization (Section 6.2) and the optimization framework (Section 6.3).

### 6.1. *Generic versus specific*

In the absence of a single segmentation algorithm capable of effectively handling all segmentation applications with satisfactory accuracy and robustness, most segmentation approaches have to deal with the delicate balance between genericity and specificity. On the one hand, generic techniques perform reasonably well over a large number of applications, mostly due to a high robustness to noise and imaging artifacts. On the other hand, application-specific methods are more accurate, the use of adapted prior knowledge increases their robustness and they can deal optimally with artifacts associated with the images they have been specifically trained on. In between these extremes, application-tailored approaches provide the user with the means to adapt an otherwise generic segmentation technique to the application at hand. For instance, the statistical shape constraint techniques we reviewed in Section 5 effectively adapt generic deformable model formulations to segment specific target structures (or a specific class of target structures).

Specialization is all the more attractive since several optimization tricks can be applied to improve the segmentation performance and speed when the application is restricted to a limited domain. In motion tracking [117] for instance, the boundaries of the segmentation target extracted at a given time may serve to initialize the segmentation of the same target at the next time instant, a tactic that relies on the assumption that the target exhibits only small changes in shape and position between time instants. Although initially developed in the context of computer vision [88,187], the most popular motion tracking application is probably the analysis of the dynamic behavior of the human heart, the left ventricle in particular [117]. The multi-channel capabilities of MR systems also motivate the increasing specialization of algorithms. Indeed, a variety of MR pulse sequences are available, where each sequence yield a different distribution of the tissue contrast characteristics. In the event where a segmentation system should be applied to images acquired with the same sequence on a single scanner, a careful study of the imaging characteristics of the sequence would most probably favor a combination of highly specific

bottom-up strategies and specifically tailored generic approaches. Conversely, it is sometimes possible to determine the optimal pulse sequence for a particular segmentation target or application [151,173]. The optimized MR acquisition processes are then specifically tuned to maximize the contrast between the tissues underlying the segmentation target and their surroundings, thereby facilitating the segmentation process.

Furthermore, real time issues and other resource constraints (CPU power, memory occupation) may severely impede the adaptation of a segmentation system from one application to another. Sophisticated model-based techniques are not particularly fast for instance and must be optimized in speed at the expense of great efforts if they are to be used in the surgical arena [210].

At any rate, segmentation systems will most probably require a large amount of specialization to become fully automated.

### 6.2. *Initialization*

As discussed throughout this chapter, the amount of noise present in the input images, the intensity inhomogeneities and imaging artifacts that plague them and the variability of the segmentation targets all contribute to a poorly structured and highly non-convex space that the segmentation system must traverse in search for the target's boundaries. Most approaches would only lead to weak sub-optimal solutions (where the deformation model adapts to noise or decoys or maybe only follows parts of the desired boundaries) if the search space were not drastically reduced by assuming that a good approximation to the solution was available. This can be either in the form of a set of pose parameters (position, orientation, scale) or shape and appearance descriptors.

Various approaches have been presented in the literature to overcome this robustness issue. Some are specific to a particular segmentation technique (histogram peak detection for region growing for instance), others (such as atlas registration) are applicable across a wider ranger of segmentation strategies.

Classification techniques often require *ad hoc* initializations. When only limited *a priori* knowledge about the characteristics of the target voxel attributes is available, in PET tumor or lesion detection applications for instance, the salient peaks in a histogram of the voxel attribute values can be used to seed region growing algorithms. Other techniques ensure relative insensitivity to seed position [206]. Note that the closely related split and merge algorithms effectively avoid this seed positioning difficulty [133,112,106]. On the other hand, when the intensity characteristics of the target structure or tissue can be statistically estimated, they can help initialize the various Gaussian means, variances and mixing coefficients of EM and Bayesian classification approaches, to ensure better classification performance [97].

In view of their inherent complexity, model-based approaches are certainly even more sensitive to initial parameters. As pointed out by Xu and Prince [217], the ini-

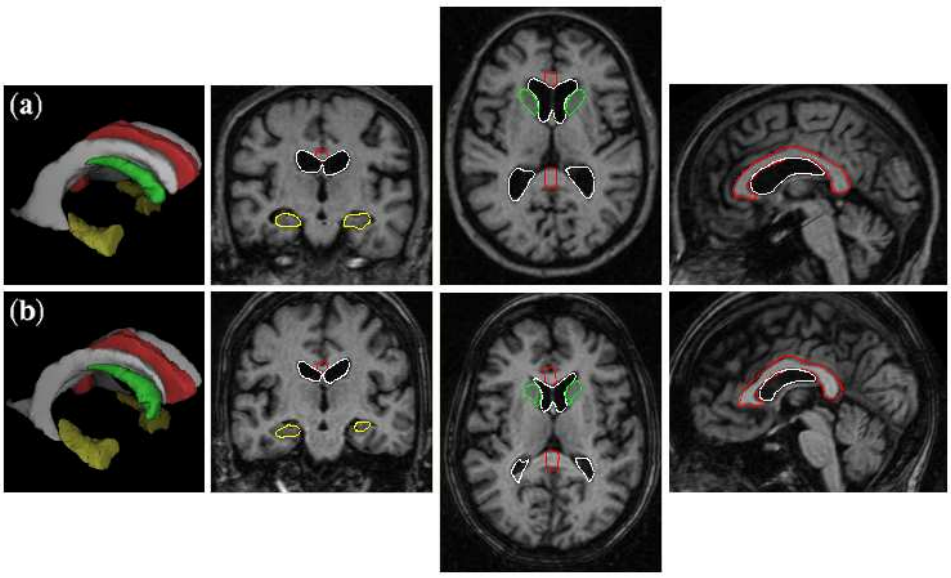


Fig. 6. (a) reference MRI with manually delineated structures superimposed (corpus callosum in red, ventricles in white, caudate nuclei in green and hippocampi in yellow); (b) reference MRI registered to an input MRI and initialized structures.

tial distance between the model and the target structure (both in terms of actual Euclidean distance and of morphological difference) and the ability to reach into concave boundaries are the two key difficulties of parametric deformable models. These have been tackled by numerous authors. Blake *et al.*[15] for instance implemented a coarse to fine strategy, the Graduated Non-Convexity Algorithm, where a scalar parameter controlled the amount of "local" convexity. To resolve the issue of the capture range of the segmentation target within a highly cluttered and tessellated environment, the models can also be initialized at a number of locations and

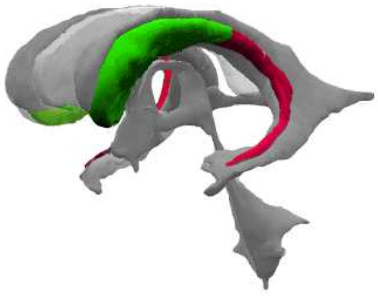

Fig. 7. Anatomically correct caudate nucleus (green + red) and manually segmented caudate nucleus (green) as obtained from most delineation protocols: the caudate tail is explicitly cut to reduce delineation variability. The nearby ventricles and corpus callosum are rendered in gray.

evolved in sequence: the deformed model with the best final match is then selected. In Pitiot *et al.*[142], a hybrid evolutionary algorithm controlled a family of deformable templates that were evolved simultaneously to explore the search space in a robust fashion. A pre-processing stage involving filtering, thresholding or morphological techniques may also be useful [223].

Yet another series of techniques utilizes linear or nonlinear registration to initialize the deformable models or the seed points of region growing approaches or level set methods reasonably close to their expected positions [162].

In Pitiot *et al.*[140], we selected an MRI brain dataset for its "standard" appearance (the reference MRI), and the target structures were carefully segmented in it (see Figure 6(a)) following established anatomic delineation protocols. Given an input MRI to be processed, the first step consisted of registering the reference MRI to it with a non-linear registration algorithm with an elastic prior (the MAMAN algorithm [24]). The transform obtained was then applied to the meshes segmented in the reference MRI. These transformed meshes served as initial guesses for the segmentation of the target structures (Figure 6(b)).

### 6.3. *Optimization scheme*

While the segmentation model determines the structure of the space of extracted shapes (see Section 4), the optimization scheme conditions the ability of the model to traverse this space in search of the correct boundaries.

Most of the segmentation approaches we have mentioned in this chapter can be cast as an optimization problem whereby the search for the target boundaries corresponds to the search for the global minimum of a given functional. The difficulties linked to the choice of a suitable segmentation criterion (which we identified in the introduction to Section 2) carry over to the determination of an adequate objective function. Namely, the remarkable variability in shape and appearance of the segmentation targets, the intensity characteristics of the input images (noise distribution, artifacts, contrasts between sutrctures, etc.) and the varying objectives of the envisioned applications all contribute to the burden of an appropriate design. However in return, formulating the segmentating process as an optimization problem clearly states its objective: finding the global minimum of the functional [f].

As with deformable models, the objective function to be minimized can be thought of as an energy, or as a sum of energies $E = \sum_i E_i$. A necessary condition to minimize $E$ is the zero crossing of its first derivative: $\nabla(E) = 0$, which

[f] In view of the somewhat irregular nature and lack of convexity of the landscape of the optimization functional, it would be illusory to expect that the global minimum would effectively coincide with the target boundaries, if it can be found at all. Yet, in practice, the many *a priori* knowledge constraints and *a priori* information imposed on the segmentation process increase the probability that a good approximation of the true boundaries coincides with a reachable local minimum not too far away from the global one.

effectively can be read as a balance of forces (with one force per energy component).

When it is not possible to minimize $E$ in a static or algebraic way, either theoretically or practically, a dynamical system can be built whose evolution to equilibrium yields the same minimum [124]. An estimation of the target boundaries can then be obtained iteratively. In fact, it is sometimes easier to directly design the laws of evolution that control such a system, most especially when some of its terms do not derive from an energy, as is often the case with medical knowledge based constraints. An added benefit is the offered possibility to converge towards the local minimum closest to the initial position. This proves useful in semi-automated segmentation systems where a manual estimate of the target boundary can be refined automatically.

However invaluable they can be in increasing the robustness to noise and imaging artifacts, these shape or appearance models induce a poorly structured optimization space when they serve as constraints on the deformation process. The matter is made worse by the high variability of the segmentation target and the tessellated nature of medical images. All in all, we are left with a very difficult minimization problem.

Several algorithms have been developed to remedy this difficulty [124], most of them coarse-to-fine strategies. In a multiscale framework [187,128] for instance, the segmentation is first performed on a smoothed downsampled version of the input image and successively refined at higher resolutions. With multiresolution techniques (pyramidal schemes), the segmentation model itself is subjected to changes in resolution (multi-scale pyramid of basis functions in Székely *et al.* [182], octree-spline in Széliski *et al.* [181], and dynamic mesh decimation in Lötjönen *et al.* [105]). Among other optimization strategies, dynamic programming was used by Amini *et al.* [2] or Coughlan *et al.* [42] to increase the spectrum of the search for the global minima. Poon *et al.* [148] selected simulated annealing, owing to its ability to reach the global minimum and to incorporate non-differentiable constraints. In Pitiot *et al.* [140], most of the parameters controlling the segmentation process were dynamically modified, along with the deformation of the models. The overall robustness was increased without sacrificing too much accuracy by dynamically controlling the balance between the two and adapting it to the segmentation problem at hand.

## 7. Validation

Characterizing, both qualitatively and quantitatively, the performances of an automated segmentation system is all the more pivotal since the available algorithms have only limited precision and accuracy. In other words, since segmentation approaches make compromises, the validity of the underlying assumptions must be checked against the envisaged applications. Yet, medical image segmentation validation is still an open problem plagued with challenges and conflicting objectives.

The foremost difficulty stems from the absence of ground truth. Given the cur-

rent resolution of the most common imaging modalities and the artifacts that afflict them, even human operators cannot establish the actual boundaries of the segmentation targets from the acquired data with sufficient accuracy. The availability of physical or simulated phantoms [178,37] partially alleviates that issue, but their limited sophistication prevents them from accurately modeling either the large anatomical complexity of organs and structures (for physical phantoms) or the full flavor of imaging characteristics (noise, inhomogeneities, partial volume effects) both in normal and pathological cases (for simulated phantoms).

Often, the target boundaries extracted by an automated algorithm are compared against those manually delineated by a series of experts, under the assumption that the expert delineations are a good approximation of the actual boundaries. However, as demonstrated by many intra- and inter- operator variability results [228,154,127,129], manual segmentation accuracy is often poor when target structures are difficult to segment, sometimes to the point where the manual delineation protocols must explicitly discard certain anatomical parts from the target structures to limit the delineation variability and avoid introducing spurious outlines (as an illustration, the segmented caudate nuclei reported in Pitiot *et al.* [140] have a very short tail, and the inferior horns of the ventricles are missing). Approaches to establish the true boundary from a series of manual delineations are being investigated [211].

What is more, the *modus operandi* of the validation studies must be adapted to the objectives of the application for which the structures are segmented in the first place. For instance, longitudinal studies typically rely more on reproductibility than actual accuracy: systematic segmentation biases may be tolerable so long as the segmentation targets are outlined consistently across a large population of input images. The ability to adequately handle pathological cases is also an application parameter that may influence the design of a segmentation approach. Consequently, although assessing the behavior of a system tuned for standard cases on pathological data is certainly informative, it would seem unfair to penalize it on such a ground. Clearly, as mentioned above, the increased robustness yielded by introducing prior medical knowledge is often counterbalanced by decreased accuracy, especially with shape models that tend to forbid the segmentation of non-standard boundaries.

The variety of segmentation objectives is clearly reflected in the diversity of validation metrics (see Zhang [222] for a broad overview). Some authors use volume overlap [53,82], or ratios of misclassified voxels [75], others the Hausdorff distance between contours [65]. Agreement measures have also been developed [225] as a means to draw a most probable decision from a set of expert ones. Unfortunately, from a practical point of view, how accuratly and easily a given validation metrics can be implemented often depends on the chosen segmentation model. This also introduces errors in the quantitative validation. For instance, the computation of the Hausdorff distance between two continuous curves or surfaces runs into quantization problems as the curves must be discretized. Furthermore, manual outlines are often obtained in the form of a set of voxels, at a somewhat coarse resolution for most radiograph-

ical modalities, which is again likely to introduce artificial errors in the validation measures.

All in all, a consensus still has to emerge as to which validation strategy to apply in each case.

## 8. Concluding remarks

With the advent of increasingly powerful and gradually less invasive modalities, medical imaging has become an invaluable tool for clinical use as well as research applications. While the quest for even better acquisition techniques continues, the attention of the medical imaging community has now shifted to the extraction of meaningful anatomical and physiological information out of the ever growing databases of medical images. Before the function, morphology or inter-relationship of organs, structures and tissues can be fully investigated, these must be isolated, that is segmented, from their embedding images. Mirroring the great variety of modalities and medical or research objectives, an even larger variety of segmentation systems has therefore been, and is still being, developed.

Yet, accurate and robust segmentation remains a challenge beset by a number of issues, that we discussed throughout this chapter. Clearly, in view of the complexity of the segmentation problem, there are no general prescriptions for selecting a "good" segmentation method. This choice must not only be driven by the characteristics of the input image (imaging artifacts, signal-to-noise ratio, contrast of the segmentation target with respect to surrounding image features, etc.) but also by the possible usage constraints (algorithmic complexity with respect to available memory/CPU resources, time limits if real-time applications are envisioned, etc.) and of course by the downstream treatments that follow this segmentation step (diagnosis, morphometric analysis, shape recognition, etc.).

However helpful automated segmentation systems could be in replacing manual operators, their limited accuracy and, more importantly, their inadequate robustness still prevent their widespread application.

In a research environment where time is less of a premium than the quality of the overall analysis, the parameters of a segmentation system can always be set to specifically fit the requirements of the envisoned application, in terms of accuracy or robustness. Furthermore, the segmentation results can be, and usually are, thoroughly checked before the actual analysis takes place. Even so, the rapid growth of image databases presses the need for fully automated tools. Because of the sheer size of the image collection to be processed, database applications are more forgiving with regard to the shortcomings of segmentation systems. Clearly, invaluable information can always be extracted even when the algorithm employed suffer from statistical biases, as long as these are consistent.

In a clinical setting though, time is a precious resource that has to be managed

tightly. To be useful, a segmentation system must exhibit maximum accuracy with the standard "out of the box" set of parameters. To gain physicians' trust, it must also be sufficiently robust not to require any exhaustive and tedious quality checking phase.

To achieve this long-term goal, substantial progress is still to be made. In the meantime, semi-automated segmentation is likely to remain the favored means to assist in the labor intensive tasks of medical imaging analysis. By assisting manual operators rather than replacing them, partial automation effectively decreases the segmentation burden without comprimising the trust placed in the quality of the final results. Semi-automated delineation tools that can complete delineations based on prior shape knowledge, atlas registration assisted segmentation systems, or expert system controlled segmentation approaches that communicate with the operator to attract his attention to potential problems, are set to obtain an increasing share of the limelight.

## References

1. A.A. Amini and J.S. Duncan. Bending and stretching models for LV wall motion analysis from curves and surfaces. *Image and Vision Computing*, 10(6):418–430, 1992.
2. A.A. Amini, T.E. Weymouth, and R.C. Jain. Using dynamic programming for solving variational problems in vision. *IEEE Transactions on Pattern Analysis and Machine Intelligence*, 12(9):855–867, 1990.
3. Y. Amit and A. Kong. Graphical templates for model registration. *IEEE Transactions on Pattern Analysis and Machine Intelligence*, 18(3):225–236, 1996.
4. N.C. Andreasen, R. Rajarethinam, T. Cizadlo, S. Arndt, V.W. Swayze II, L.A. Flashman, D.S. O'Leary, J.C. Ehrhardt, and W.T.C. Yuh. Automatic atlas-based volume estimation of human brain regions from MR images. *Journal of Computer Assisted Tomography*, 20(1):98–106, 1996.
5. E. Ardizzone, D. Peri, R. Pirrone, A. Palma, and G. Peri. Knowledge based Approach to Intelligent Data Analysis of Medical Images. In *Proc. of Intelligent Data Analysis in Medicine and Pharmacology (IDAMAP'02)*, 2001.
6. N. Ayache, P. Cinquin, I. Cohen, L. Cohen, F. Leitner, and O. Monga. Segmentation of complex three dimensional medical objects: a challenge and a requirement for computer-assisted surgery planning and performance. In *Computer Integrated Surgery: Technology and Clinical Applications*, pages 59–74. 1996.
7. K.T. Bae, M.L. Giger, C. Chen, and C.E. Kahn. Automatic segmentation of liver structure in CT images. *Medical Physics*, 20(1):71–78, 1993.
8. R. Bajcsy and S. Kovacic. Multiresolution elastic matching. *Computer Vision, Graphics, and Image Processing*, 46:1–21, 1989.
9. P. Baldi and S. Brunak. *Bioinformatics. The Machine Learning Approach.* MIT Press, 1998.
10. E. Bardinet, L. Cohen, and N. Ayache. Tracking and motion analysis of the left ventricle with deformable superquadrics. *Medical Imaging analysis*, 1(2):129–149, 1996.
11. V. Barra and J.Y. Boire. Automatic Segmentation of Subcortical Brain Structures in MR Images Using Information Fusion. *IEEE Transactions on Medical Imaging*, 20(7):549–558, 2001.
12. R. Bernard, B. Lika, and F. Pernus. Segmenting Articulated Structures by Hierar-

chical Statistical Modeling of Shape, Appearance, and Topology. In *Proc. of Medical Image Computing and Computer-Assisted Intervention (MICCAI'01)*, pages 499–506, 2001.

13. J. Besag. Spatial Interaction and the Statistical Analysis of Lattice Systems. *Journal of the Royal Statistical Society*, 36:344–348, 1974.
14. J.C. Bezdek, L.O. Hall, and L.P. Clarke. Review of MR image segmentation techniques using pattern recognition. *Medical Physics*, 20:1033–1048, 1993.
15. A. Blake and A. Zisserman. *Visual Reconstruction*. MIT Press, 1987.
16. R.E. Blanton, J.L. Levitt, P.M. Thompson, L.F. Capetillo-Cunliffe, T. Sadoun, T. Williams, J.T. McCracken, and A.W. Toga. Mapping Cortical Variability and Complexity Patterns in the Developing Human Brain. *Psychiatry Research*, 107(1):29–43, 2001.
17. T.O. Blum. *Transformation for Extracting New Descriptors of Shape. Models for the Perception of Speech and Visual Form*. MIT Press, 1967.
18. E. Borenstein, E. Sharon, and S. Ullman. Combining Top-Down and Bottom-Up Segmentation. In *Proc. of Computer Vision and Pattern Recognition (CVPR'04)*, 2004.
19. G. Borgefors. Distance transformations in arbitrary dimensions. *Computer Vision, Graphics, and Image Processing*, 27:321–345, 1984.
20. C. Brechbühler. *Description and Analysis of 3-D Shapes by Parameterization of Closed Surfaces*. Ph.d. thesis, IKT/BIWI, ETH ETH Zürich, 1995.
21. M. Brejl and M. Sonka. Object Localization and Border Detection Criteria Design in Edge-Based Image Segmentation: Automated Learning from Examples. *IEEE Transactions on Medical Imaging*, 19(10):973–985, 2000.
22. M.S. Brown, L.S. Wilson, B.D. Doust, R.W. Gill, and C. Sun. Knowledge-based Method for Segmentation and Analysis of Lung Boundaries in Chest X-ray Images. *Computerized Medical Imaging and Graphics*, 22:463–477, 1998.
23. E. Bullmore, M. Brammer, G. Rouleau, B. Everitt, and A. Simmons. Computerized brain tissue classification of magnetic resonance images: a new approach to the problem of partial volume artifact. *Neuroimage*, 2:133–147, 1995.
24. P. Cachier, E. Bardinet, D. Dormont, X. Pennec, and N. Ayache. Iconic Feature Based Nonrigid Registration: The PASHA Algorithm. *CVIU — Special Issue on Nonrigid Registration*, 89(2-3):272–298, Feb.-march 2003.
25. A. Chakraborty, L.H. Staib, and J.S. Duncan. Deformable boundary finding in medical images by integrating gradient and region information. *IEEE Transactions on Medical Imaging*, 15(6):859–870, 1996.
26. C.H. Chen and G.G. Lee. On digital mammogram segmentation and microcalcification detection using multiresolution wavelet analysis. *Graphical Models and Image Processing*, 59(5):349–364, 1997.
27. Y. Chen, H.D. Tagare, M. Rado, D. wilson, and E.A. Geiser. Using prior shape and intensity profile in medical image segmentation. In *Proc. of International Conference on Computer Vision (ICCV'03)*, pages 1117–11123, 2003.
28. S.M. Choi, J.E. Lee, J. Kim, and M.H. Kim. Volumetric objection reconstruction using the 3D-MRF model-based segmentation. *IEEE Transactions on Medical Imaging*, 16:887–892, 1997.
29. G.E. Christensen, S.C. Joshi, and M.I. Miller. Volumetric transformation of brain anatomy. *IEEE Transactions on Medical Imaging*, 16:864–877, 1997.
30. M.C. Clark, L.O. Hall, D.B. Goldgof, L.P. Clarke, R.P. Velthuizen, and M.S. Silbiger. MRI segmentation using fuzzy clustering techniques. *IEEE Engineering in Medicine and Biology Magazine*, pages 730–742, 1994.

31. M.C. Clark, L.O. Hall, D.B. Goldgof, R. Velthuizen, and F.R. Murtagh. Automatic tumor segmentation using knowledge-based techniques. *IEEE Transactions on Medical Imaging*, pages 187–201, 1998.
32. L.P. Clarke, R.P. Velthuizen, M.A. Camacho, J.J. Heine, and M. Vaidyanathan. MRI segmentation: methods and applications. *Magnetic Resonance Imaging*, 12(3):343–368, 1995.
33. I. Cohen, N. Ayache, and P. Sulget. Tracking Points on Deformable Objects using Curvature Information. In *Proc. of European Conference on Computer Vision (ECCV'92)*, pages 458–466, 1992.
34. I. Cohen and L.D. Cohen. Hyperquadric model for 2D and 3D data fitting. In *Proc. of International Conference on Pattern Recognition (ICPR'94)*, pages 403–405, 1994.
35. L.D. Cohen and I. Cohen. Finite element methods for active contour models and balloons for 2D and 3D images. *Transactions on Pattern Analysis and Machine Intelligence*, 15(11):1131–1147, 1993.
36. D. Collins, C. Holmes, T. Peters, and A. Evans. Automatic 3D model-based neuroanatomical segmentation. *Human Brain Mapping*, 3(3):190–208, 1995.
37. D. Collins, A. Zijdenbos, V. Kollokian, J. Sled, N. Kabani, C. Holmes, and A. Evans. Design and Construction of a Realistic Digital Brain Phantom. *IEEE Transactions on Medical Imaging*, 26(3):463–468, 1998.
38. D. L. Collins, A. P. Zijdenbos, T. Paus, and A. C. Evans. Use of registration for cohort studies. In Joseph Hajnal, David Hawkes, and Derek Hill, editors, *Medical Image Registration*. Kluwer, 2003.
39. T.F. Cootes, D.H. Cooper, C.J. Taylor, and J. Graham. Trainable method of parametric shape description. *Image Vision Computing*, 10(5):289–294, 1992.
40. T.F. Cootes, G.J. Edwards, and C.J. Taylor. Active Appearance Models. In *Proc. of European Conference on Computer Vision (ECCV'98)*, pages 484–498, 1998.
41. Timothy F. Cootes, A. Hill, Christopher J. Taylor, and J. Haslam. Use of Active Shape Models for Locating Structures in Medical Images. *Image and Vision Computing*, 12(6):355–366, 1994.
42. J. Coughlan, A. Yuille, C. English, and D. Snow. Efficient Deformable Template Detection and Localization without User Initialization. *Computer Vision and Image Understanding*, 78(3):303–319, 2000.
43. T.M. Cover and J.M. Van Campenhout. On the possible orderings in the measurement selection problem. *IEEE Transactions on Systems Man and Cybernetics*, 7:657–661, 1977.
44. C. Davatzikos. Spatial normalization of 3D images using deformable models. *Journal of Computer Assisted Tomography*, 20(4):656–665, 1996.
45. C. Davatzikos and R.N. Bryan. Using a deformable surface model to obtain a shape representation of the cortex. *IEEE Transactions on Medical Imaging*, 15(6):785–795, 1996.
46. C. Davatzikos, J. Prince, and N. Bryan. Image Registration Based on Boundary Mapping. *IEEE Transactions on Medical Imaging*, 15(1):212–215, 1996.
47. C. Davatzikos, M. Vaillant, S. Resnick, J.L. Prince, S. Letovsky, and R.N. Bryan. Computerized Method for Morphological Analysis of the Corpus Callosum. *Journal of Computer Assisted Tomography*, 20:88–97, 1998.
48. R.H. Davies, C.J. Twining, T.F. Cootes, J.C. Waterton, and C.J. Taylor. A Minimum Description Length Approach to Statistical Shape Modelling. *IEEE Transactions on Medical Imaging*, 21(5):525–537, 2002.
49. A.C. Davison. *Statistical Models*. Cambridge Press, 2003.
50. R. Deklerck, J. Cornelis, and M. Bister. Segmentation of medical images. *Image and*

*Vision Computing*, 11(8):486–503, 1993.
51. H. Delingette. General object reconstruction based on simplex meshes. *International Journal of Computer Vision*, 32(2):111–146, 1999.
52. H. Delingette and J. Montagnat. Shape and topology constraints on parametric active contours. *Computer Vision and Image Understanding*, 83(2):140–171, 2001.
53. L.R. Dice. Measures of the amount of ecologic association between species. *Ecology*, 26(3):297–302, 1945.
54. R.O. Duda, E. Hart, and D.G. Stork. *Pattern Classification (second edition)*. Wiley-Interscience, 2000.
55. J.S. Duncan, X. Papademetris, J. Yang, M. Jackowski, X. Zeng, and L.H. Staib. Geometric Strategies for Neuroanatomic Analysis from MRI. *Neuroimage*, 2004. to appear.
56. M. Egmont-Petersen, D. de Ridder, and H. Handels. Image processing with neural networks - a review. *Pattern Recognition*, 35(10):2279–2301, 2002.
57. Bruce Fischl, David H. Salat, Evelina Busa, Marilyn Albert, Megan Dieterich, Christian Haselgrove, Andre van der Kouwe, Ron Killiany, David Kennedy, Shuna Klaveness, Albert Montillo, Nikos Makris, Bruce Rosen, and Anders M. Dale. Whole Brain Segmentation: Automated Labeling of Neuroanatomical Structures in the Human Brain. *Neuron*, 33:341–355, 2002.
58. M. Fischler and R. Elschlager. The Representation and Matching of Pictorial Structures. *IEEE Transactions on Computers*, 22(1):67–92, 1973.
59. M. Fleuté, S. Lavallée, and R. Julliard. Incorporating a Statistically Based Shape Model into a System for Computer-Assisted Anterior Cruciate Ligament Surgery. *Medical Image Analysis*, 3(3):209–222, 1999.
60. A.S. Frangakis, A. Stoschek, and R. Hegerl. Wavelet transform filtering and nonlinear anisotropic diffusion assessed for signal reconstruction performance on multidimensional biomedical data. *IEEE Transactions on Biomedical Engineering*, 48(2):213–222, 2001.
61. T.O.J. Fuchs, M. Kachelriess, and W.A. Kalender. Fast volume scanning approaches by X-ray-computed tomography. *Proceedings of the IEEE*, 91(10):1492–1502, 2003.
62. J. Gao, A Kosaka, and A. Kak. A Deformable Model for Human Organ Extraction. In *Proc. of International Conference on Image Processing (ICIP'98)*, volume 3, pages 323–327, 1998.
63. Y. Ge, J.M. Fitzpatrick, B.M. Dawant, J. Bao, R.M. Kessler, and R. Margolin. Accurate localization of cortical convolutions in MR brain images. *IEEE Transactions on Medical Imaging*, 15:418–428, 1996.
64. S. Geman and D. Geman. Stochastic relaxation, Gibbs distributions and the Bayesian restoration of images. *IEEE Transactions on Pattern Analysis and Machine Intelligence*, 6:721–741, 1984.
65. G. Gerig, M. Jomier, and M. Chakos. Valmet: A New Validation Tool for Assessing and Improving 3D Object Segmentation. In *Proc. of Medical Image Computing and Computer-Assisted Intervention (MICCAI'01)*, pages 516–528, 2001.
66. P. Gibbs, D.L. Buckley, S.J. Blackband, and A. Horsman. Tumour volume detection from MR images by morphological segmentation. *Physics in Medicine and Biology*, 41(11):2437–2446, 1996.
67. P. Golland, W.E.L. Grimson, M.E. Shenton, and R. Kikinis. Deformation Analysis for Shape Based Classification. In *Proc. of Information Processing in Medical Imaging (IPMI'01)*, pages 517–530, 2001.
68. C.L. Gordon, C.E. Webber, J.D. Adachi, and N. Christoforou. In vivo assessment of trabecular bone structure at the distal radius from high-resolution computed tomog-

raphy images. *Physics in Medicine and Biology*, 41:495–508, 1996.
69. J. Green. *Medical Image Processing: The Mathematics of Medical Imaging*. Greenwood Research, 2001.
70. R. Gupta and P.E. Undrill. The use of texture analysis to delineate suspicious masses in mammograhy. *Physics in Medicine and Biology*, 40(5):835–855, 1995.
71. L.O. Hall, A.M. Bensaid, and L.P. Clarke. A comparison of neural network and fuzzy clustering techniques in segmenting magnetic resonance images of the brain. *Neural Networks*, 3(5):672–682, 1992.
72. S.M. Haney, P.M. Thompson, T.F. Cloughesy, J.R. Alger, and A.W. Toga. Tracking tumor growth rates in patients with malignant gliomas: A test of two algorithms. *American Journal of Neuroradiology*, 22(1):73–82, 2001.
73. R.M. Haralick and L.G. Shapiro. Image segmentation techniques. *Computer Vision, Graphics and Image Processing*, 29:100–132, 1985.
74. T.J. Hebert. Fast iterative segmentation of high resolution medical images. *IEEE Transactions on Nuclear Science*, 44:1363–1367, 1997.
75. K. Held, E.R. Kops, B.J. Krause, W.M. Wells, R. Kikinis, and H. Müller-Gärtner. Markov random field segmentation of brain MR images. *IEEE Transactions on Medical Imaging*, 16(6), 1997.
76. R.C. Herndon, J.L. Lancaster, A.W. Toga, and P.T. Fox. Quantification of white matter and gray matter volumes from T1 parametric images using fuzzy classifiers. *Journal of Magnetic Resonance Imaging*, 6:425–435, 1996.
77. S. Ho, E. Bullitt, and G. Gerig. Level set evolution with region competition: Automatic 3D segmentation of brain tumors. In *Proc. of International Conference on Pattern Recognition (ICPR'02)*, pages 532–535, 2002.
78. L.T. Holly and K.T. Foley. Intraoperative spinal navigation. *Spine*, 28(15):554–561, 2003.
79. L. Holmstrom, P. Koistinen, J. Laaksonen, and E. Oja. Neural and statistical classifiers-taxonomy and two case studies. *IEEE Transactions on Neural Networks*, 8(1):5–17, 1997.
80. J. Hug, C. Brechbühler, and G. Székely. Model-based Intitialisation for Segmentation. In *Proceedings of European Conference on Computer Vision (ECCV'00)*, 2000.
81. N. Ibrahim, H. Fujita, T. Hara, and T. Endo. Automated detection of clustered microcalcifications on mammograms: CAD system application to MIAS database. *Physics in Medicine and Biology*, 42:2577–2589, 1997.
82. P. Jaccard. The distribution of flora in the alpine zone. *New Phytologist*, 11:37–50, 1912.
83. A.K. Jain and B. Chandrasekaran. Dimensionality and sample size considerations. In P.R. Krishnaiah and L.N. Kanal, editors, *Pattern Recognition Practice*, volume 2, pages 835–855. 1982.
84. A.K. Jain and D. Zongker. Feature Selection: Evaluation, Application, and Small Sample Performence. *IEEE Transactions on Pattern Analysis and Machine Intelligence*, 19(2):153–158, 1997.
85. S. Joshi, M. Miller, and U. Grenander. On the Geometry and Shape of Brain Sub-Manifolds. *Pattern Recognition and Artificial Intelligence*, 11:1317–1343, 1997.
86. S. Joshi, S. Pizer, P.T. Fletcher, A. Thall, and G. Tracton. Multi-scale 3-D Deformable Model Segmentation Based on Medial Description. In *Proc. of Information Processing in Medical Imaging (IPMI'01)*, pages 64–77, 2001.
87. T. Kanungo, D.M. Mount, N.S. Netanyahu, C.D. Piatko, R. Silverman, and A.Y. Wu. An efficient k-means clustering algorithm: analysis and implementation. *IEEE Transactions on Pattern Analysis and Machine Intelligence*, 24(7):881–892, 2002.

88. M. Kass, A. Witkin, and D. Terzopoulos. Snakes: Active contour models. *International Journal of Computer Vision*, 1(4):321–331, 1988.
89. A. Kelemen, G. Székely, and G. Gerig. Three-Dimensional Model-based Segmentation of Brain MRI. *IEEE Transactions on Medical Imaging*, 18(10):838–849, 1999.
90. V.S. Khoo, D.P. Dearnaley, D.J. Finnigan, A. Padhani, S.F. Tanner, and M.O. Leach. Magnetic resonance imaging (MRI): considerations and applications in radiotherapy treatment planning. *Radiotherapy and Oncology*, 42(1):1–15, 1997.
91. R. Kruse, J. Gebhart, and F. Klawonn. *Foundations of Fuzzy Systems*. Wiley, 1994.
92. M.A. Kupinski and M.L. Giger. Automated seeded lesion segmentation on digital mammograms. *IEEE Transactions on Medical Imaging*, 17:510–517, 1998.
93. J.L. Lancaster, L.H. Rainey, J.L. Summerlin, C.S. Freitas, P.T. Fox, A.C. Evans, A.W. Toga, and J.C. Mazziotta. Automated labeling of the human brain: A preliminary report on the development and evaluation of a forward-transform method. *Human Brain Mapping*, 5:238–242, 1997.
94. S.M. Lawrie and S.S. Abukmeil. Brain abnormality in schizophrenia: a systematic and quantitative review of volumetric magnetic resonance image studies. *Journal of Psychiatry*, 172:110–120, 1998.
95. C. Lee, S. Hun, T.A. Ketter, and M. Unser. Unsupervised connectivity-based thresholding segmentation of midsagittal brain MR images. *Computer Biology Medicine*, 28:309–338, 1998.
96. S.U. Lee, S.Y. Chung, and R.H. Park. A comparative performance study of several global thresholding techniques for segmentation. *Computer Vision, Graphics, and Image Processing*, 52:171–190, 1990.
97. K. Van Leemput, F. Maes, D. Vandermeulen, and P. Suetens. Automated model-based tissue classification of MR images of the brain. *IEEE transactions on Medical Imaging*, 18(10):897–908, 1999.
98. T.M. Lehmann, C. Gonner, and K. Spitzer. Survey: interpolation methods in medical image processing. *IEEE Transactions on Medical Imaging*, 18(11):1049–1075, 1999.
99. J.M. Leski. Generalized weighted conditional fuzzy clustering. *IEEE Transactions on Fuzzy Systems*, 11(6):709–715, 2003.
100. M. Leventon, E. Grimson, and O. Faugeras. Statistical Shape Influence in Geodesic Active Contours. In *Proc. of Computer Vision and Pattern Recognition (CVPR'00)*, pages 4–11, 2000.
101. H. Li, R. Deklerck, B. De Cuyper, A. Hermanus, E. Nyssen, and J. Cornelis. Object Recognition in Brain CT-Scans: Knowledge-Based Fusion of Data from Multiple Feature Extractors. *IEEE Transactions on Medical Imaging*, 14(2):212–229, 1995.
102. Z. Liang. Tissue classification and segmentation of MR images. *IEEE Engineering in Medicine and Biology Magazine*, 12(1):81–85, 1993.
103. Z. Liang, J.R. MacFall, and D.P. Harrington. Parameter estimation and tissue segmentation from multispectral MR images. *IEEE Transactions on Medical Imaging*, 13:441–449, 1994.
104. P. Lipson, A.L. Yuille, D. O'Keefe, J. Cavanaugh, J. Taaffe, and D. Rosenthal. Deformable Templates for Feature Extraction from Medical Images. In *Proceedings of First European Conference on Computer Vision (ECCV'90)*, pages 477–484, 1990.
105. J. Lotjonen, P.-J. Reissman, I. Magnin, and T. Katila. Model extraction from magnetic resonance volume data using the deformable pyramid. *Medical Image Analysis*, 3(4):387–406, 1999.
106. Y.L. Lu, T.Z. Jiang, and Y.F. Zang. Split-merge based region growing method for fMRI activation detection. *Human Brain Mapping*, 2004. in press.
107. A. Macovski. *Medical imaging systems*. Prentice-Hall, 1938.

108. S. Malassiotis and M.G. Strintzis. Tracking the left ventricle in echocardiographic images by learning heart dynamics. *IEEE Transactions on Medical Imaging*, 18(2):282–290, 1999.
109. R. Malladi, J. Sethian, and B.C. Vemuri. Shape modeling with front propagation: a level set approach. *IEEE Transactions on Pattern Analysis and Machine Intelligence*, 17(2):158–175, 1995.
110. R. Malladi, J.A. Sethian, and B.C. Vemuri. A fast level set based algorithm for topology-independent shape modeling. *Journal of Mathematical Imaging and Vision*, 6:269–289, 1996.
111. J.F. Mangin, V. Frouin, I. Bloch, J. Regis, and J. Lopez-Krahe. From 3D magnetic resonance images to structural representations of the cortex topography using topology preserving deformations. *Journal of Mathematical Imaging and Vision*, 5:297–318, 1995.
112. I.N. Manousakas, P.E. Undrill, G.G. Cameron, and T.W. Redpath. Split-and-merge segmentation of magnetic resonance medical images: performance evaluation and extension to three dimensions. *Computers and Biomedical Research*, 31(6):393–412, 1998.
113. K.V. Mardia and T.J. Hainsworth. A spatial thresholding method for image segmentation. *IEEE Transactions on Pattern Analysis and Machine Intelligence*, 10(6):919–927, 1988.
114. D. Marr and H.K. Nishihara. Visual Information Processing: Artificial Intelligence and the Sensorium of Sight. *Technology Review*, 81(1):2–23, 1978.
115. M. Matesin, S. Loncaric, and D. Petravic. A Rule-Based Approach to Stroke Lesion Analysis from CT Brain Images. In *Proc. of Second International Symposium on Image and Signal Processing and Analysis*, pages 219–223, 2001.
116. W. Maurel, Y. Wu, N. Magnenat Thalmann, and D. Thalmann. *Biomechanical Models for Soft Tissue Simulation*. Springer Verlag, 1998.
117. T. McInerney and D. Terzopoulos. Deformable Models in Medical Image Analysis: A Survey. *Medical Image Analysis*, 1(2):91–108, 1996.
118. T. McInerney and D. Terzopoulos. T-snakes: topology adaptive snakes. *Medical Image Analysis*, (4):73–91, 2000.
119. G.J. McLachlan and T. Krishnan. *The EM Algorithm and Extensions*. John Wiley and Sons, 1997.
120. D. Metaxas and D. Terzopoulos. Shape and Nonrigid Motion Estimation through Physics-Based Synthesis. *IEEE Transactions on Pattern Analysis and Machine Intelligence*, 15(6):580–591, 1993.
121. I. Mikic, S. Krucinski, and J.D. Thomas. Segmentation and tracking in echocardiographic sequences: active contours guided by optical flow estimates. *IEEE Transactions on Medical Imaging*, 17:274–284, 1998.
122. J.V. Miller, D.E. Breen, W.E. Lorensen, R.N. O'Bara, and M.J. Wozny. Geometrically deformed models: a method for extracting closed geometric models from volume data. In *Proc. of SIGGRAPH'91*, pages 217–226, 1991.
123. J. Montagnat and H. Delingette. Globally constrained deformable models for 3D object reconstruction. *Signal Processing*, 71(2):173–186, 1998.
124. J. Montagnat, H. Delingette, and N. Ayache. A review of deformable surfaces: topology, geometry and deformation. *Image and Vision Computing*, 19:1023–1040, 2001.
125. J. Montagnat, H. Delingette, N. Ayache, J.M. Clément, C. Roy, Y. Russier, V. Tassetti, and J. Marescaux. Liver segmentation in contrast enhanced helical ct-scans. In *Proc. of World Congress on Medical Physics and Biomedical Engineering*, 1997.
126. Y. Nakagawa and A. Rosenfeld. Some experiments on variable thresholding. *Pattern*

*Recognition*, 11:191–204, 1979.
127. K.L. Narr, P.M. Thompson, T. Sharma, J. Moussai, A.F. Cannestra, and A.W. Toga. Mapping Morphology of the Corpus Callosum in Schizophrenia. *Cerebral Cortex*, 10(1):40–49, 2000.
128. W. J. Niessen, K. L. Vincken, J. Weickert, B. M. Ter Haar Romeny, and M. A. Viergever. Multiscale Segmentation of Three-Dimensional MR Brain Images. *International Journal of Computer Vision*, 31(2):185–202, 1999.
129. A. Obenaus, C.J. Yong-Hing, K.A. Tong, and G.E. Sarty. A Reliable Method for Measurement and Normalization of Pediatric Hippocampal Volumes. *Pediatric Research*, 50:124–132, 2001.
130. S. Osher and J.A. Sethian. Fronts Propagating with Curvature-Dependent Speed: Algorithms Based on Hamilton–Jacobi Formulations. *Journal of Computational Physics*, 79:12–49, 1988.
131. B. O'Sullivan and J. Shah. New TNM staging criteria for head and neck tumors. *Semin. Surf. Oncol.*, 21(1):30–42, 2003.
132. X. Papademetris, A.J. Sinusas, D.P. Dione, R.T. Constable, and J.S. Duncan. Estimation of 3-D left ventricular deformation from medical images using biomechanical models. *IEEE Transactions on Medical Imaging*, 21(7):786–800, 2002.
133. J.M. Pardo, D. Cabello, and J. Heras. Automatic 3D shape reconstruction of bones. In *Proc. of Engineering in Medicine and Biology Society*, pages 387–388, 1995.
134. J.M. Pardo, D.Cabello, and J.Heras. A snake for model-based segmentation of biomedical images. *Pattern Recognition Letters*, 18:1529–1538, 1997.
135. J.M. Pardo-Lopez, D. Cabello, J. Heras, and J. Couceiro. A Markov random field model for bony tissue classification. *Computerized Medical Imaging and Graphics*, 22:169–178, 1998.
136. J. Park, D. Metaxas, and L. Axel. Analysis of left ventricular wall motion based on volumetric deformable models and MRI-SPAMM. *Medical Image Analysis*, 1(1), 1996.
137. D.L. Pham and J.L. Prince. An adaptive fuzzy c-means algorithm for image segmentation in the presence of intensity inhomogeneities. *Pattern Recognition Letters*, pages 57–68, 1999.
138. D.L. Pham, C. Xu, and J.L. Prince. Current Methods in Medical Image Segmentation. *Annual Review of Biomedical Engineering, Annual Reviews*, 2:315–337, 1996.
139. A. Pitiot. *Automated Segmentation of Cerebral Structures Incorporating Explicit Knowledge*. PhD thesis, Ecole des Mines de Paris, 2003.
140. A. Pitiot, H. Delingette, P.M. Thompson, and N. Ayache. Expert Knowledge Guided Segmentation System for Brain MRI. *Neuroimage*, 2004. to appear.
141. A. Pitiot, H. Delingette, A. Toga, and P. Thompson. Learning object correspondences with the observed transport shape measure. In *Proc. of Information Processing in Medical Imaging IPMI'03*, 2003.
142. A. Pitiot, A.W. Toga, and P.M. Thompson. Adaptive Elastic Segmentation of Brain MRI via Shape-Model-Guided Evolutionary Programming. *IEEE Transactions on Medical Imaging*, 21(8):910–923, 2002.
143. S.M. Pizer, D.S. Fritsch, P. Yushkevich, V. Johnson, and E.L. Chaney. Segmentation, Registration, and Measurement of Shape Variation via Image Object Shape. *IEEE Transactions on Medical Imaging*, 10(18):851–865, 1999.
144. S.M. Pizer, M.R. Jiroutek, C. Lu, K.E. Muller, G. Tracton, P. Yushkevich, E.L. Chaney, P.T. Fletcher, S. Joshi, A. Thall, J.Z. Chen, Y. Fridman, D.S. Fritsch, A.G. Gash, and J.M. Glotzer. Deformable M-Reps for 3D Medical Image Segmentation. *International Journal of Computer Vision*, 55(2), 2003.

145. T. Poggio and V. Torra. Ill-posed Problems and Regularization Analysis in Early Vision. In *Proceedings of AARPA Image Understanding Workshop*, pages 257–263, 1984.
146. S. Pohlman, K.A. Powell, N.A. Obuchowski, W.A. Chilcote, and S. Grundfest-Broniatowski. Quantitative classification of breast tumors in digitized mammograms. *Medical Physics*, 23:1337–1345, 1996.
147. W.E. Polakowski, D.A. Cournoyer, S.K. Rogers, M.P. DeSimio, D.W. Ruck, J.W. Hoffmeister, and R.A. Raines. Computer-aided breast cancer detection and diagnosis of masses using difference of Gaussians and derivative-based feature saliency. *IEEE Transactions on Medical Imaging*, 16:811–819, 1997.
148. C.S. Poon, M. Braun, R. Fahrig, A. Ginige, and A. Dorrell. Segmentation of medical images using an active contour model incorporating region-based image features. In R.A. Robb, editor, *Visualisation in Biomedical Computing*, pages 90–97. 1994.
149. F. Poupon, J.-F. Mangin, D. Hasboun, Industrial Metrology, and V. Frouin. Multi-object Deformable Templates Dedicated to the Segmentation of Brain Deep Structures. In *Proc. of Medical Image Computing and Computer-Assisted Intervention (MICCAI'98)*, pages 1134–1143, 1998.
150. C.E. Priebe, D.J. Marchette, and G.W. Rogers. Segmentation of random fields via borrowed strength density estimation. *IEEE Transactions on Pattern Analysis and Machine Intelligence*, 19:494–499, 1997.
151. J.L. Prince, Q. Tan, and D. Pham. Optimization of MR pulse sequences for Bayesian image segmentation. *Medical Physics*, 22:1651–1656, 1995.
152. J. Rademacher, A.M Galaburda, D.N. Kennedy, P.A. Filipek, and V.S. Caviness. Human cerebral cortex: localization, parcellation and morphometry with magnetic resonance imaging. *Journal of Cognitive Neuroscience*, 4:352–374, 1992.
153. J.C. Rajapakse, J.N. Giedd, and J.L. Rapoport. Statistical approach to segmentation of single-channel cerebral MR images. *IEEE Transactions on Medical Imaging*, 16:176–186, 1997.
154. R. A. Rauch and J. R. Jinkins. Variability of corpus callosal area measurements from midsagittal MR images: effect of subject placement within the scanner. *American Journal of Neuroradiology*, 17(1):27–28, 1996.
155. W.E. Reddick, J.O. Glass, E.N. Cook, T.D. Elkin, and R.J. Deaton. Automated segmentation and classification of multispectral magnetic resonance images of brain using artificial neural networks. *IEEE Transactions on Medical Imaging*, 16:911–918, 1997.
156. A.L. Reiss, J.G. Hennessey, M. Rubin, L. Beach, M.T. Abrams, I. Warsofsky, M.-C. Liu, and J.M. Links. Reliability and validity of an algorithm for fuzzy tissue segmentation of MRI. *Journal of Computer Assisted Tomography*, 22:471–479, 1998.
157. D. Rey, G. Subsol, H. Delingette, and N. Ayache. Automatic Detection and Segmentation of Evolving Processes in 3D Medical Images: Application to Multiple Sclerosis. *Medical Image Analysis*, 6(2):163–179, 2002.
158. M.R. Rezaee, P.M.J. van der Zwet, B.P.E. Lelieveldt, R.J. van der Geest, and J.H.C. Reiber. A A multiresolution image segmentation technique based on pyramidal segmentation and fuzzy clustering. *IEEE Transactions on Image Processing*, 9(7):1238–1248, 2000.
159. D. Rivière, J.-F. Mangin, D. Papadopoulos-Orfanos, J.-M. Martinez, V. Frouin, and J. Régis. Automatic recognition of cortical sulci of the Human Brain using a congregation of neural networks. *Medical Imaging Analysis*, 6(2):77–92, 2002.
160. P.K. Sahoo, S. Soltani, and A.K.C.Wong. A survey of thresholding techniques. *Computer Vision, Graphics and Imaging Processing*, 41:233–260, 1988.

161. S. Sandor and R. Leahy. Towards automatic labelling of the cerebral cortex using a deformable model. In *Proc. of Information Processing in Medical Imaging (IPMI'95)*, 1995.
162. S. Sandor and R. Leahy. Surface-based labeling of cortical anatomy using a deformable atlas. *IEEE Transactions on Medical Imaging*, 16:41–54, 1997.
163. B. Sankur and M. Sezgin. A Survey Over Image Thresholding Techniques And Quantitative Performance Evaluation. *Journal of Electronic Imaging*, 13(1):146–165, 2004.
164. G. Sapiro, R. Kimmel, and V. Caselles. Object detection and measurements in medical images via geodesic deformable contours. *Vision Geometry IV*, pages 366–378, 1995.
165. A. Sebbahi, A. Herment, A. deCesare, and E. Mousseaux. Multimodality cardiovascular image segmentation using a deformable contour model. *Computerized Medical Imaging and Graphics*, 21:79–89, 1997.
166. M. Sermesant, C. Forest, X. Pennec, H. Delingette, and N. Ayache. Deformable biomechanical models: Application to 4d cardiac image analysis. *Medical Image Analysis*, 7(4):475–488, December 2003.
167. J.A. Sethian. *Level Set Methods: Evolving Interfaces in Geometry, Fluid Mechanics, Computer Vision and Materials Sciences*. Cambridge University Press, 1996.
168. D. Shen, E.H. Herskovits, and C. Davatzikos. An adaptive-focus statistical shape model for segmentation and shape modeling of 3-D brain structures. *IEEE Transactions on Medical Imaging*, 20(4):257–270, 2001.
169. A. Simmons, P.S. Tofts, G.J. Barker, and S.R. Arridge. Sources of intensity nonuniformity in spin echo images at 1.5T. *Magnetic Resonance Medicine*, 32:121–128, 1994.
170. H.R. Singleton and G.M. Pohost. Automatic cardiac MR image segmentation using edge detection by tissue classification in pixel neighborhoods. *Magnetic Resonance Medicine*, 37:418–424, 1997.
171. J.G. Sled and G.B. Pike. Standing-wave and RF penetration artifacts caused by elliptic geometry: an electrodynamic analysis of MRI. *IEEE Transactions on Medical Imaging*, 17:653–662, 1998.
172. S.M. Smith, N. De Stefano, M. Jenkinson, and P.M. Matthews. Normalised accurate measurement of longitudinal brain change. *Journal of Computer Assisted Tomography*, 25(3):466–475, 2001.
173. H. Soltanian-Zadeh, R. Saigal, J.P. Waindham, A.E. Yagle, and D.O Hearshen. Optimization of MRI protocols and pulse sequence parameters for eigenimage filtering. *IEEE Transactions on Medical Imaging*, 13(1):161–175, 1994.
174. P. Sprawls. *Physical principles of medical imaging*. Aspen Publishers, 1993.
175. L.H. Staib and J.S. Duncan. Boundary Finding with Parametrically Deformable Models. *IEEE Transactions on Pattern Analysis and Machine Intelligence*, 14(11):1061–1075, 1992.
176. J. Stoeckel, G. Malandain, O. Migneco, P.M. Koulibaly, P. Robert, N. Ayache, and J. Darcourt. Classification of SPECT Images of Normal Subjects versus Images of Alzheimer's Disease Patients. In *Proc. of Medical Image Computing and Computer-Assisted Intervention (MICCAI'01)*, pages 666–674, 2001.
177. C. Studholme, D. L. G. Hill, and D. J. Hawkes. Incorporating connected region labelling into automated image registration using mutual information. In *IEEE Workshop on Mathematical Methods in Biomedical Image Analysis (MMBIA'96)*, pages 23–31. IEEE Computer Society Press, 1996.
178. M. Styner, C. Brechbuhler, G. Székely, and G. Gerig. Parametric estimate of intensity inhomogeneities applied to MRI. *IEEE Transactions on Medical Imaging*, 19:152–165,

2000.

179. M. Styner and G. Gerig. Medial Models Incorporating Object Variability for 3-D Shape Analysis. In *Proceedings of Information Processing in Medical Imaging (IPMI'01)*, pages 502–516, 2001.
180. J.S. Suri, L. Kecheng, S. Singh, S.N. Laxminarayan, Z. Xialoan, and L. Reden. Shape recovery algorithms using level sets in 2-D/3-D medical imagery: a state-of-the-art review. *IEEE Transactions on Information Technology in Biomedicine*, 6(1):8–28, 2002.
181. R. Szeliski and S. Lavallee. Matching 3-d anatomical surfaces with non-rigid deformations using octree-splines. *International Journal of Computer Vision*, 18(2):171–186, 1996.
182. G. Székely, A. Kelemen, C. Brechbühler, and G. Gerig. Segmentation of 2-D and 3-D Objects from MRI Volume Data using Constrained Elastic Deformations of Flexible Fourier Surface Models. *Medical Image Analysis*, 1(1):19–34, 1996.
183. J. Talairach and P. Tournoux. *Co-Planar Stereotaxic Atlas of the Human Brain. 3-Dimensional Proportional System: An Approach to Cerebral Imaging.* Thieme Medical Publisher, Stuttgart, 1988.
184. G. Taubin, C. Fernando, S. Sullivan, J. Ponce, and D.J. Kriegman. Parameterized Families of Polynomials for bounded Algebraic Curve and Surface Fitting. *IEEE Transactions on Pattern Analysis and Machine Intelligence*, 16(3):287–303, 1994.
185. P. Taylor. Computer aids for decision-making in diagnostic radiology - a literature review. *Brittish Journal of Radiology*, 68:945–957, 1995.
186. H. Tek and B.B. Kimia. Volumetric segmentation of medical images by three-dimensional bubbles. *Computer Vision and Image Understanding*, 65:246–258, 1997.
187. D. Terzopoulos and K. Fleischer. Deformable models. *The Visual Computer*, 4(6):306–331, 1988.
188. P.M. Thompson, M.S. Mega, R.P. Woods, C.I. Zoumalan, C.J. Lindshield, R.E. Blanton, J. Moussai, C.J. Holmes, J.L. Cummings, and A.W. Toga. Cortical Change in Alzheimer's Disease Detected with a Disease-specific Population-based Brain Atlas. *Cerebral Cortex*, 11(1):1–16, 2001.
189. P.M. Thompson, J. Moussai, S. Zohoori, A. Goldkorn, A.A Khan, M.S. Mega, G.W. Small, J.L. Cummings, and A.W. Toga. Cortical Variability and Asymmetry in Normal Aging and Alzheimer's Disease. *Cerebral Cortex*, 8(6):492–509, 1998.
190. P.M. Thompson, K.L. Narr, R.E. Blanton, and A.W. Toga. Mapping Structural Alterations of the Corpus Callosum during Brain Development and Degeneration. In E. Zaidel and M. Iacoboni, editors, *The Corpus Callosum*. MIT Press, 2003.
191. P.M. Thompson, C. Schwartz, and A.W. Toga. High-Resolution Random Mesh Algorithms for Creating a Probabilistic 3D Surface Atlas of the Human Brain. *Neuroimage*, 3(1):19–34, 1996.
192. P.M. Thompson and A.W. Toga. Detection, Visualisation and Animation of Abnormal Anatomic Structure with a Deformable Probabilistic Brain Atlas Based on Random Vector Field Transformations. *Medical Image Analysis*, 1(4):271–294, 1997.
193. P.M. Thompson, R.P. Woods, M.S. Mega, and A.W. Toga. Mathematical/Computational Challenges in Creating Deformable and Probabilistic Atlases of the Human Brain. *Human Brain Mapping*, 9(2):81–92, 2000.
194. A.W. Toga. *Brain Warping*. Academic Press, 1998.
195. D. Tosun, M.E. Rettmann, X. Han, X. Tao, C. Xu, S.M. Resnick, D. Pham, and J.L. Prince. Cortical Surface Segmentation and Mapping. *Neuroimage*, 2004. to appear.
196. A. Trouvé and L. Younes. Diffeomorphic Matching Problems in One Dimension: Designing and Minimizing Matching Functionals. In *Proc. of European Conference*

*on Computer Vision (ECCV'00)*, pages 573–587, 2000.
197. A. Tsai, W. Wells, C. Tempany, E. Grimson, and A. Willsky. Coupled Multi-shape Model and Mutual Information for Medical Image Segmentation. In *Proceedings of Information Processing in Medical Imaging (IPMI'03)*, pages 185–197, 2003.
198. M. Turk and A. Pentland. Eigenfaces for recognition. *Journal of Cognitive Neuroscience*, 3(1):71–86, 1991.
199. J.K. Udupa and P.K. Saha. Fuzzy connectedness and image segmentation. *Proceedings of the IEEE*, 91(10):1649–1669, 2003.
200. D. Vandermeulen, R. Verbeeck, L. Berben, D. Delaere, P. Suetens, and G. Marchal. Continuous voxel classification by stochastic relaxation: theory and application to MR imaging and MR angiography. *Image and Vision Computing*, 12:559–572, 1994.
201. M. Vasilescu and D. Terzopoulos. Adaptive meshes and shells: irregular triangulation, discontinuities and hierarchical subdivision. In *Proc. of Computer Vision and Pattern Recognition (CVPR'92)*, pages 829–832, 1992.
202. B. C. Vemuri, Y. Guo, C. M. Leonard, and S-H. Lai. Fast numerical algorithms for fitting multiresolution hybrid shape models to brain MRI. *Medical Image Analysis*, 1(1):343–362, 1997.
203. B.C. Vemuri, A. Radisavljevic, and C. Leonard. Multiresolution 3-D Stochastic Hybrid Shape Models for Image Segmentation. In *Proceedings of Information Processing in Medical Imaging (IPMI'93)*, pages 62–76, 1993.
204. D.L. Vilarino, V.M. Brea, D. Cabello, and J.M. Pardo. Discrete-time CNN for image segmentation by active contours. *Pattern Recognition Letters*, 19:721–734, 1998.
205. N.F. Vittitoe, R. Vargas-Voracek, and C.E. Floyd. Identification of lung regions in chest radiographs using Markov random field modeling. *Medical Physics*, 25:976–985, 1998.
206. S.-Y. Wan and W.E. Higgins. Symmetric region growing. *IEEE Transactions on Image Processing*, 12(9):1007–1015, 2003.
207. S.-Y. Wan and E. Nung. Seed-invariant region growing: its properties and applications to 3-D medical CT images. In *Proc. of International Conference on Image Processing (ICIP'01)*, 2001.
208. Y. Wang, T. Adali, and S.Y. Kung. Quantification and segmentation of brain tissues from MR images - a probabilistic neural network approach. *IEEE Transactions on Image Processing*, 7(8):1165–1181, 1998.
209. Y. Wang, B.S. Peterson, and L.H. Staib. Shape-Based 3D Surface Correspondence using Geodesics and Local Geometry. In *Proc. of Computer Vision and Pattern Recognition (CVPR'00)*, pages 644–651, 2000.
210. S.K. Warfield, F.A. Jolesz, and R. Kikinis. Real-Time Image Segmentation for Image-Guided Surgery. In *Proc. of Conference on High Performance Networking and Computing*, page 42, 1998.
211. S.K. Warfield, K.H. Zou, and W.M. Wells. Validation of Image Segmentation and Expert Quality with an Expectation-Minimization Algorithm. In *Proc. of Medical Image Computing and Computer-Assisted Intervention (MICCAI'02)*, pages 298–306, 2002.
212. W.M. Wells, W.E.L. Grimson, R. Kikins, and F.A. Jolesz. Adaptive segmentation of MRI data. *IEEE Transactions on Medical Imaging*, 15:429–442, 1996.
213. H.H. Wen, W.C. Lin, and C.T. Chen. Knowledge-Based Medical Image Registration. In *Proceedings of the IEEE Engineering in Medicine and Biology Society*, pages 1200–1201, 1996.
214. P.J. Werbos. *The roots of backpropagation: from ordered derivatives to neural networks and political forecasting.* Wiley, 1994.

215. R. Whitaker. Volumetric deformable models. In *Proc. of Visualization in Biomedical Computing (VBC'94)*, 1994.
216. A.J. Worth and D.N. Kennedy. Segmentation of magnetic resonance brain images using analogue constraint satisfaction neural networks. *Image Vision Computing*, 12(6):345–354, 1994.
217. C. Xu and J. Prince. Snakes, Shapes and Gradient Vector Flow. *IEEE Transactions on Image Processing*, 7(3):359–369, 1998.
218. J. Yang, L.H. Staib, and J.S. Duncan. Neighbor-Constrained Segmentation with 3D Deformable Models. In *Proceedings of Information Processing in Medical Imaging (IPMI'03)*, pages 198–209, 2003.
219. A. Yezzi, S. Kichenassamy, A. Kumar, P. Olver, and A. Tannenbaum. A geometric snake model for segmentation of medical imagery. *IEEE Transactions on Medical Imaging*, 16:199–209, 1997.
220. Z. Yue, A. Goshtasby, and L.V. Ackerman. Automatic detection of rib borders in chest radiographs. *IEEE Transactions on Medical Imaging*, 14:525–536, 1995.
221. A.L Yuille, P.W. Hallinan, and D.S. Cohen. Feature Extraction from Faces using Deformable Templates. *International Journal of Computer Vision*, 8:99–111, 1992.
222. Y.J. Zhang. A survey on evaluation methods for image segmentation. *Pattern Recognition Letters*, 29:1335–1346, 1996.
223. L. Zhukov, K. Museth, D. Breen, R. Whitaker, and A.H. Barr. Level Set Modeling and Segmentation of DT-MRI Brain Data. *Journal of Electronic Imaging*, 12(1):125–133, 2003.
224. A.P. Zijdenbos and B.M. Dawant. Brain segmentation and white matter lesion detection in MR images. *Critical Reviews in Biomedical Engineering*, 22:401–465, 1994.
225. A.P. Zijdenbos, B.M. Dawant, R.A. Margolin, and A.C. Palmer. Morphometric Analysis of White Matter Lesions in MR Images: Method and Validation. *IEEE Transactions on Medical Imaging*, 13:716–724, 1994.
226. Y. Zimmerand, R. Tepper, and S. Akselrod. A two-dimensional extension of minimum cross entropy thresholding for the segmentation of ultrasound images. *Ultrasound in Medicine and Biology*, 22:1183–1190, 1996.
227. R.A. Zoroofi, Y. Sato, T. Sasama, T. Nishii, N. Sugano, K. Yonenobu, H. Yoshikawa, T. Ochi, and S. Tamura. Automated segmentation of acetabulum and femoral head from 3-D CT images. *IEEE Transactions on Information Technology in Biomedicine*, 7(4):329–343, 2003.
228. K.H. Zou, W.M. Wells, M. Kaus, R. Kikinis, F.A. Jolesz, and S.K. Warfield. Statistical Validation of Automated Probabilistic Segmentation against Composite Latent Expert Ground Truth in MR Imaging of Brain Tumors. In *Proc. of Medical Image Computing and Computer-Assisted Intervention (MICCAI'02)*, pages 315–322, 2002.